




Aptamer and nanomaterial based FRET biosensors: a review on recent advances (2014–2019)

Zeki Semih Pehlivan¹ · Milad Torabfam¹ · Hasan Kurt^{2,3} · Cleva Ow-Yang¹ · Niko Hildebrandt⁴ · Meral Yüce⁵ 

Received: 5 March 2019 / Accepted: 2 July 2019 / Published online: 24 July 2019
© Springer-Verlag GmbH Austria, part of Springer Nature 2019

Abstract

Fluorescence resonance energy transfer, one of the most powerful phenomena for elucidating molecular interactions, has been extensively utilized as a biosensing tool to provide accurate information at the nanoscale. Numerous aptamer- and nanomaterial-based FRET bioassays have been developed for detection of a large variety of molecules. Affinity probes are widely used in biosensors, in which aptamers have emerged as advantageous biorecognition elements, due to their chemical and structural stability. Similarly, optically active nanomaterials offer significant advantages over conventional organic dyes, such as superior photophysical properties, large surface-to-volume ratios, photostability, and longer shelf life. In this report (with 175 references), the use of aptamer-modified nanomaterials as FRET couples is reviewed: quantum dots, upconverting nanoparticles, graphene, reduced graphene oxide, gold nanoparticles, molybdenum disulfide, graphene quantum dots, carbon dots, and metal-organic frameworks. Tabulated summaries provide the reader with useful information on the current state of research in the field.

Keywords Biosensors · ssDNA · FRET · Up-converting nanoparticles · Quantum dots · Gold nanoparticles · Graphene · Graphene quantum dots · Carbon dots · Reduced graphene oxide · Metal-organic framework

Introduction

The so-called Förster resonance energy transfer (FRET; also referred to as *fluorescence resonance energy transfer*) was, first described at around 1950 and has strongly improved the sensing capabilities of fluorometry. It is characterized by rapid response and multiplexing capability even in small sample

volumes [1, 2]. FRET is a non-radiative energy transfer process that occurs over nanometer scale separations (up to 10 nm) between an emitter (donor) and an absorber molecule (acceptor), often called a “FRET pair”. If this donor-acceptor pair is correctly oriented and luminescence spectrum of the donor overlaps with the absorption spectrum of the acceptor, energy can be transferred non-radiatively. This energy transfer leads to luminescence quenching of emission from donor and FRET-sensitized acceptor pairs, when the acceptor is luminescent [3].

Several critical parameters should be considered when designing a FRET pair. Both the rate of FRET (k_{FRET}) and the FRET efficiency (E_{FRET}) vary directly with the distance separating the FRET pair (R), the luminescence quantum yield of the donor molecule in the absence of the acceptor (Φ_D), the spectral overlap of the donor emission profile and acceptor absorption profile (J), and the luminescence lifetime of the donor (τ_D) [4]. As shown in the Eqs. 1–4 [5, 6] and Fig. 1 [7], FRET reaches its maximum efficiency when R is smaller than R_0 , which is the donor-acceptor distance corresponding to an efficiency of 50%, and the FRET

✉ Meral Yüce
meralyuce@sabanciuniv.edu

¹ Faculty of Engineering and Natural Sciences, Sabanci University, 34956, Tuzla, Istanbul, Turkey

² School of Engineering and Natural Sciences, Istanbul Medipol University, 34810, Beykoz, Istanbul, Turkey

³ Nanosolar Plasmonics Ltd, 41400, Gebze, Kocaeli, Turkey

⁴ NanoBioPhotonics (nanofret.com), Institute for Integrative Biology of the Cell (I2BC), Université Paris-Saclay, Université Paris-Sud, CNRS, CEA, 91400 Orsay, France

⁵ SUNUM Nanotechnology Research and Application Centre, Sabanci University, 34956, Tuzla, Istanbul, Turkey

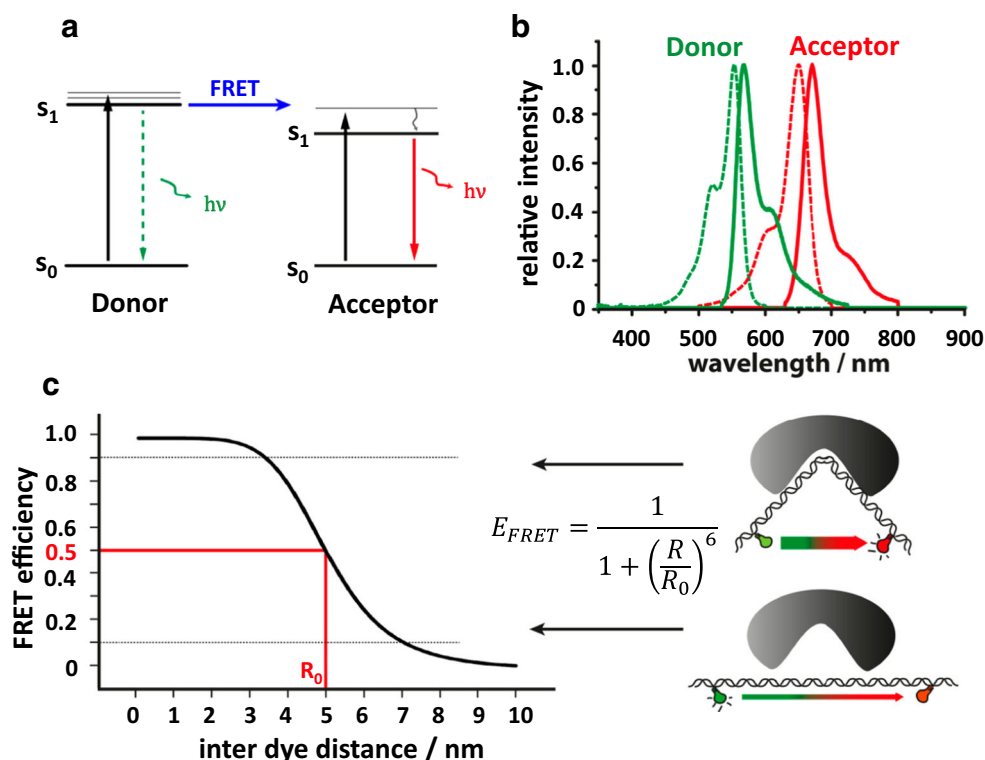


Fig. 1 Fundamental FRET principles: **(a)** A simplified energy level scheme represents the excitation of the donor from a ground state to an excited state. A donor fluorophore in proximity to an acceptor, initially in its excited state, may transfer energy to an acceptor through the non-radiative dipole-dipole coupling (blue arrow). This additional energy pathway causes faster luminescence decay of the donor (dotted arrow) and excitation of the acceptor in energetic resonance. If the acceptor is also a fluorophore, sensitization by FRET from the donor can lead to

acceptor luminescence (red arrow); **(b)** spectral overlap between emission spectrum of a donor dye (green continuous line, Alexa Fluor 555) and absorption spectrum of an acceptor dye (red dashed line, Alexa Fluor 647) that leads to FRET; **(c)** FRET efficiency (E_{FRET}) as a function of donor-acceptor distance (taking a Förster radius R_0 as 5 nm). Adapted from reference [7], which is an open-access article distributed under the Creative Commons Attribution 4.0 International License

efficiency decreases with R^{-6} . Hence, FRET occurs only over very short distances, i.e., up to 10 nm. Dependence of FRET on separation distance enables the conversion of near-field detection to a far-field signal that produces high detection sensitivity, even for small concentrations of analyte [8]. The rate of FRET can be described as.

$$k_{D \rightarrow A} = \left(\frac{1}{\tau_D} \right) \times \left(\frac{R_0}{R} \right)^6 \quad (1)$$

where τ_D is the luminescence lifetime of the donor, R is the separation distance between the donor and the acceptor, and R_0 is the Förster distance. The Förster distance is defined as.

$$R_0 = \left(\frac{9(\ln 10) \kappa^2 \Phi_D}{128 N_A \pi^5 n^4} J \right)^{\frac{1}{6}} \quad (2)$$

where κ^2 is the orientation factor of donor and acceptor dipoles, Φ_D the luminescence quantum yield of the donor,

and n the refractive index of the surrounding environment. Spectral overlap of donor emission and acceptor absorption is accordingly determined by.

$$J = \int J(\lambda) d\lambda = \int F_D(\lambda) \lambda^4 \epsilon_A(\lambda) d\lambda \quad (3)$$

where F_D is the normalized photoluminescence emission of the donor, ϵ_A the spectral extinction coefficient of the acceptor, and λ the wavelength [9]. Finally, FRET efficiency can be reduced to.

$$E_{FRET} = \frac{k_{D \rightarrow A}}{k_{D \rightarrow A} + \tau_D^{-1}} = \frac{R_0^6}{R_0^6 + R^6} \quad (4)$$

Nanomaterials as energy donors offer significant advantages over conventional dyes for FRET applications. Several nanoparticles are associated with the quantum confinement effect, which can provide tunable optoelectronic properties through control of their size and shape during synthesis. Accordingly, they show narrow emission profiles with high quantum yields, which can result in higher FRET efficiencies

over conventional dyes [10]. Acceptor-type nanomaterials offer efficient quenching, as widely reported for gold nanoparticles (AuNPs) – in this case, the energy transfer is called NSET for nanosurface energy transfer — and graphene oxide (GO) [11, 12]. FRET acceptors combine efficient quenching with tunable FRET-sensitized emissions for multiplexed detection that requires specific FRET-donors, such as lanthanide complexes, bio/chemiluminescent molecules or upconverting nanoparticles (UCNPs) [13]. Mechanical, electronic, structural, physical and chemical properties arising from high surface area density make nanoparticles highly desirable components for detection applications [14–17]. To use nanomaterials in FRET assays, one must control the distance between donor and acceptor molecules. Intermolecular interactions between donors and acceptors should be sufficiently strong to render them a FRET couple, yet weak enough to allow their disassociation in the presence of a target molecule or analyte [18]. Additionally, selectivity for the desired analyte should be achievable at luminescence intensities that are sufficient for reliable detection. To overcome such design and response limitations, there are different target-specific affinity probes already available in the market.

Antibodies and aptamers are the most commonly used affinity probes in biosensing applications, due to well established selectivity toward their targets. Antibodies are attractive affinity probes for protein-based analyte detection studies. However, existing antibodies are mostly produced *in vivo*, where batch to batch quality often fluctuates, rendering them expensive and difficult to implement. Antibodies have a short shelf-life and low tolerance to changes in environmental conditions, such as buffer, pH or temperature. Moreover, the amino acid components of antibodies are bulky and show limited variation in secondary structure [19], restricting their utility in FRET biosensors, where molecular flexibility is essential to manage the distance between participating molecules. Aptamers are short and can be found as synthetic RNA, single-stranded DNA (ssDNA) or peptide chains. They show superior chemical stability over antibodies, because they are synthesized by solid-phase chemical reactions. In contrast to antibodies, aptamers are much smaller in size and have rich and reversible secondary structure conformations. Moreover, they can be labeled and tailored chemically for any desired nucleotide point [20–22], which provides an essential advantage in FRET to control the distance between acceptor and donor molecules. The advantages of aptamers have greatly expanded their utilization as affinity probes in FRET-based biological applications.

FRET assays are usually split into two types as turn/switch/signal-ON and turn/switch/signal-OFF assays. As introduced above and illustrated in Fig. 2, bringing an acceptor and a donor molecule into close proximity results in FRET under certain conditions. Before introducing an analyte into an assay environment, fluorescent (donor) molecule can be entirely

quenched by the acceptor, leading to a significant decrease in the overall emission signal of the donor. In the presence of an analyte, aptamer-modified FRET partner prefers to bind to the corresponding analyte because of the higher selectivity and affinity. Finally, optimal distance condition between the FRET couple is broken, resulting in the recovery of the luminescence signal that is theoretically proportional to the analyte concentration. In this type of “signal-on” FRET assays, the fluorescent signal increases in the presence of the analyte. By contrast, in the case of “signal-OFF” methods, the overall fluorescent signal of donor decreases by the increase in the amount of analyte molecule [23, 24]. Herein, the recent advances in aptamer and nanomaterial-based FRET biosensors are reviewed. General properties of aptamer-modified nanomaterials employed as donor (quantum dots, up-conversion nanoparticles, graphene quantum dots, and metal-organic frameworks) and acceptor molecules (quantum dots, graphene, graphene oxide, reduced graphene oxide and gold nanoparticles) in FRET assays are discussed in detail by giving examples from the current literature.

Aptamers in FRET

Aptamers are selected *in vitro* from random oligonucleotide pools of DNA or RNA molecules through the method, known as “Systematic Evolution of Ligands by EXponential Enrichment” (SELEX) [25]. They are capable of binding to target molecules with high affinity and specificity. Aptamers can be in two or more structural conformations, such as hairpin shape, loop or a hybridized form upon target binding. These properties make aptamers ideal identification elements in the development of biosensors [20, 26, 27]. Aptamers have critical advantages such as thermal and chemical stability, large-scale chemical production, controlled *in vitro* selection, low immunogenicity and target versatility [20]. These advantages make aptamers alternative diagnostic and therapeutic tools for future biomedical applications in comparison with the antibody-based detection methods. Aptamers can be selected from sizeable combinatorial oligonucleotide pools against a wide range of target analytes such as proteins [28], heavy metals [29], bacteria [30] and nanomaterials [31]. It is worth mentioning that aptamers are certain materials for diverse areas, not only as alternatives to antibodies but also as the fundamental parts in scientific and medical equipment. Aptasensor is a type of sensor which depends on target-specific aptamers as the central detection element [32]. A variety of aptamer-based methodologies have been reported so far, including electrochemical biosensors [33], fluorescence-based optical aptasensors [26] and colorimetric aptasensors [34].

Aptamers are non-fluorescent (in the visible) like other nucleic acids. Thus, post-selection modifications with external fluorophores has to be performed to convert aptamers into

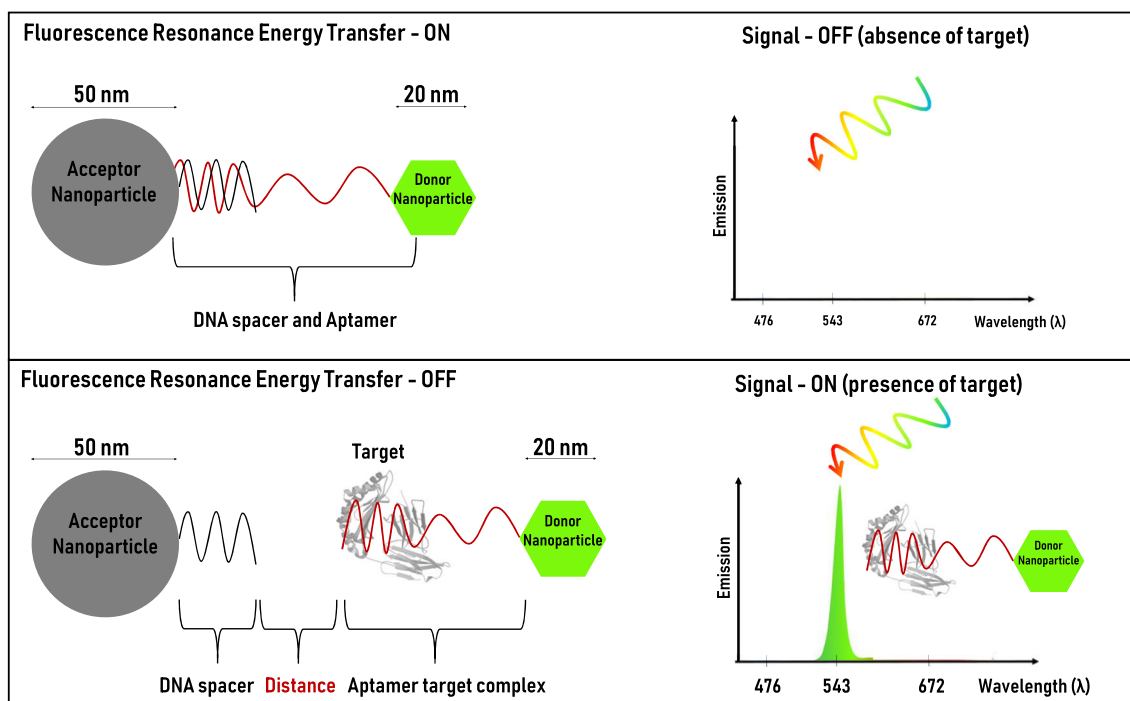


Fig. 2 Schematic representation of a Fluorescence Resonance Energy Transfer based aptamer nanoprobe in the absence and presence of a given target molecule. Structures not drawn to their original scales

visibly fluorescent signalling reporters. Detection is related to the disparity in fluorescence properties of a molecular identification part when it interacts with the target [3]. Researchers use nano-fluorophores, such as QDs or UCNPs as labels for aptamer modification. Change of fluorescence intensity or anisotropy, resulting from the change of the rotational motion of the fluorophore, plays a vital role in a target-aptamer binding in the single fluorophore-labeled type of aptamers. In FRET assays, aptamers act as excavators that mainly seek the target analytes from a complex sample with the aim of binding. Also during the process of binding, intermolecular and intramolecular FRET between the donor and acceptor molecules gives rise to higher sensitivity [35], due to the considerably small size of aptamers (10–50 kDa) in comparison to full-size antibodies (around 150 kDa). Consequently, aptamer-based FRET assays can be developed to detect various analytes like large (bacteria) and small molecules (ions and nucleic acids), according to aptamers available in the market. Several factors influence the sensitivity of aptamer-based FRET assays; for example, the degree of combination with the target, the number of fluorophores integrated with the aptamer, the closeness of the fluorophore and the quencher molecules [36]. It should be noted that the coupling of aptamers with nanomaterials can enhance the nuclease resistance of the oligonucleotides, further protecting them from renal filtration, due to increased size; on the other hand, antibody-nanomaterial pairs usually do not encounter such limitations, owing to their greater molecular weight (around 150 kDa) and better pharmacokinetic properties [20]. Additional chemical modifications are also

available in the market, for instance, the use of 2'-fluoro- or 2'-amino-substituted pyrimidines or 2'-O-methyl nucleotides during oligo synthesis, to enable oligonucleotides to withstand against potential nuclease attacks in serum [37].

Having a distinct variety in 2D/3D conformations before and after binding with the target is one of the salient features of aptamers. In particular, aptamers are used as a bridge in between FRET donor and acceptors, and their critical feature is in their secondary structure, the so-called “hairpin”. The loop part in hairpin structures is formed through non-complementary nucleobases interactions. In the presence of an analyte, on the other hand, the chain elongates when the Watson-Crick pair is broken to form a bond with an analyte, which brings the FRET acceptor and donor out of proximity for energy transfer, resulting in the turn-on signal. A counter example is one in which the hairpin structure forms in the presence of an analyte, such as that occurring in small analyte detection cases like ions [38]. The hairpin structure was well employed by Ghosh et al. [39] to detect glycosylated albumin (GA). According to that study, QDs, and AuNPs coupled to each end of the GA-selective aptamer, forming a hairpin structure in the absence of the target due to the guanine content. Consequently, FRET couple stayed in sufficient proximity for transfer of the excited donor energy, which led quenching of the signal by AuNPs. On the other hand, the broken structure of the hairpin in the presence of target brought the FRET probes out of proximity and led to the recovery of the QD signal. A limit of detection (LoD) of ca. 1 nM was achieved by this secondary structure-based FRET aptasensor [39].

Another distinctive 3D conformation, Nanopyramids, are self-assembled, complex 3D aptamer structures that contain FRET acceptor or donor molecules at each corner of the pyramid. As a structure formed by short aptamers, donors and acceptors located at the corners are close enough to support resonant energy transfer. Hence, all fluorescence emitted by the donors is quenched effectively by the acceptors. However, in the presence of an analyte, which is a complementary nucleic acid chain, the 3D structure of the aptamers is destroyed, due to the higher affinity of one or more aptamer towards the target. Consequently, turn-on sensing is achieved upon the liberation of the donor molecules [40]. Nanotweezers are another type of self-assembled 3D structure, in which FRET donor and acceptor molecules are bound to the corners of the nanostructure. He et al. [2] demonstrated fabricated tetrahedron nanotweezers that offered the dual advantages of aptamer structural versatility and control over the binding points of aptamers. In the absence of an analyte, which was a tumor-related mRNA, the acceptor and donor were separated far enough to suppress energy transfer via the aptamer structure holding them together. Hence, fluorescence was observed. However, when the analyte was introduced, the 3D aptamer structure was deformed, bringing the acceptors and donors into closer proximity that resulted in FRET. Quenching occurred, and turn-off detection was achieved.

Through direct modification with fluorophores, the structural conversion of aptamers has a significant impact on the participating FRET molecules. During the binding process, the signal alteration can indicate the spatial separation range, either by increasing (i.e., the “signal-on” mode) or by decreasing (i.e., the “signal-off” mode). In the “signal-on” biosensor of fluorescently-labeled aptamers, one end of the aptamer is connected to a fluorophore, where a quencher later blocks its fluorescence signal during energy transfer. Upon separation of the fluorophore and the quencher (through target binding), the fluorescence signal is recovered, thereby enabling qualitative and quantitative detection of the target concentration [41]. Figures of merit for detection can generally be quantified and evaluated by an LoD and dynamic detection range. Limit of detection, or detection limit, represents the lowest amount of analyte that can be detected with statistical confidence. Dynamic detection range (dynamic range or linear range), on the other hand, indicates the range between the lowest and highest amount of analyte that can be quantified. FRET can also be applied for “signal-off” type assay construction, which is usually less sensitive than those based on the “signal-on” principle. Signal-off methods occasionally result in better detection of targets with high-affinity aptamers. However, “signal-off” types are labor-saving and cost-effective due to their simpler design. In general, a fluorescence donor and an acceptor molecule are connected to either end of the aptamer. Target binding is followed by a structural change of the aptamer, which induces the donor and quencher in

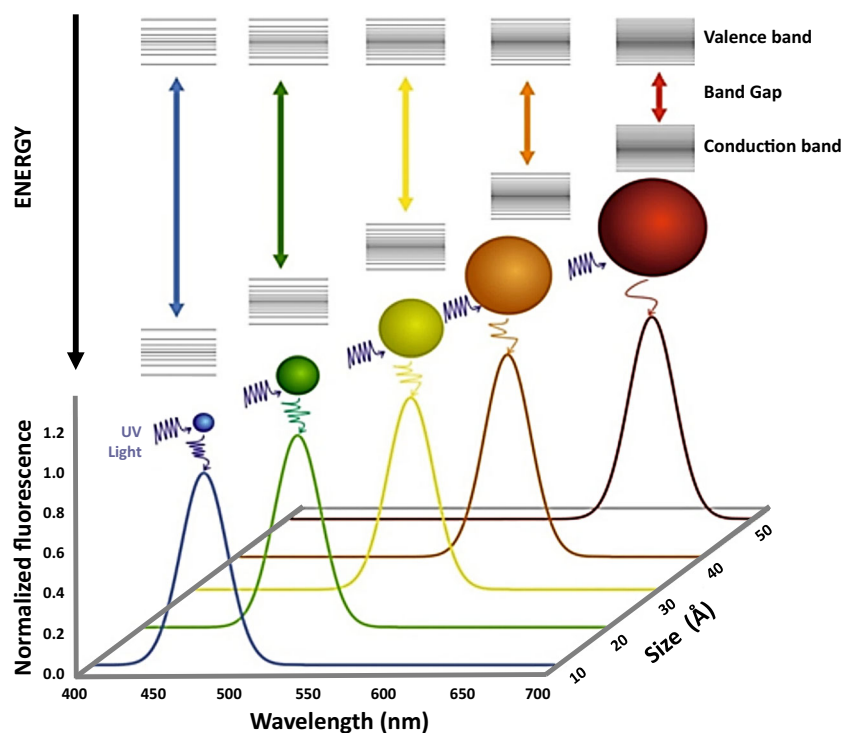
proximity. This phenomenon causes fluorescence quenching [42]. Besides modifying probe materials, chemical interactions can also be tuned by the structural change of the aptamers. The thrombin aptamer, for instance, is a guanine-rich ssDNA sequence that forms an intramolecular quadruplex structure upon target binding [37]. Recently, more exotic nanomaterials have been used for aptamer-based thrombin detection: graphene, which acts as an acceptor [43], upconverting nanophosphors, carbon nanoparticles [44], and quantum dots (QDs) [37]. In addition, a considerable number of different analytes were also detected by use of aptamers and nanomaterials, including Carcinoembryonic antigen (CEA) [45], PSA [46], different types of bacteria [42], as well as drugs such as theophylline [47] and cocaine [48]. Those nanomaterials, coupled with target-specific aptamers in FRET assays are comprehensively discussed in the next section.

Nanomaterials as detection probes in FRET-based aptasensors

Semiconductor Quantum Dots (QDs)

Choosing a donor material with high quantum yield is a critical factor for achieving high FRET rates. As reported in many studies, the use of organic dyes as donor materials in conventional FRET systems suffers from photo-bleaching [38]. This issue motivates the growing emergence of photo-stable inorganic materials with the high quantum yield for energy transfer-based applications. QDs provide a convenient solution to this problem as a result of their stable physicochemical properties [13]. The energy levels of QDs are discontinuous and confined by their small size. Absorption and emission spectra of QDs can be tailored from the near-infrared (NIR) to ultraviolet (UV), as represented in Fig. 3 [49], with extensive absorption, narrow emission spectra and high quantum yield [50]. These parameters enable QDs as efficient FRET donors. From the structure perspective, commonly used QDs can be classified as core and core/shell types. The core-type QDs are synthesized through encapsulation by organic surfactants. This method of quantum confinement causes defects on the QD surface, which act as traps and lead to a decrease in the luminescence quantum yield [51]. Nonetheless, core-type QDs can provide enough luminescence intensity for effective energy transfer and are still being used for energy transfer-based applications. To overcome the limitation of core-type QDs, a semiconductor shell structure is introduced to the QDs. In core/shell-type QD structures, dangling bonds of the semiconductor shell material are used to confine or encapsulate the QD [52]. As a result, better QD/shell interface and charge transfer in between the layers are achieved, and improved quantum yields warrant higher luminescence intensities.

Fig. 3 Revealing a number of apparent differences among optical emissions of binary CdSe and ternary CdSeTe QDs at different sizes. The dependence of emission wavelength on the size of nanoparticles enables developing tunable emission throughout the visible region. Adapted from reference [49], which is an open-access article distributed under the Creative Commons Attribution 4.0 International License



CdSe@ZnS is a typical core/shell QD structure that has been employed in small molecule detection applications, such as Pb^{2+} [41] and antigens [53]. Although the high quantum yield makes QDs attractive for such platforms, the toxic nature of these nanoparticles is the major challenge for biological applications [54]. With their heavy metal composition, QDs like CdSe and CdTe have been gradually abandoned. To address this problem, for example, Zhang et al. [55] used cadmium-free Mn^{2+} -doped ZnS QDs as a donor for FRET-based detection of different proteins, and they achieved a detection limit of 5 ng/ml for biotin and streptavidin interaction. In a similar approach, Arvand et al. [56] detected Edifenphos fungicide with metal-free ZnS QDs.

Apart from the toxicity issue, QD-based FRET methods suffer from background noise, due to their excitation energy occurring in the spectral range of biological autofluorescence. Duan et al. [57] solved this problem with an elegant FRET design based on dual QD donors: red-emitting QDs (rQD) and green-emitting QDs (gQD). In that study, rQDs were expressly chosen to avoid autofluorescence in the spectra. gQDs, on the other hand, were used to balance the fluorescence intensity against the rapid decrease in the fluorescence intensity of rQDs. As a result, sufficient signal intensity was achieved with an improved signal-to-background ratio using a dual QD-donor FRET system. For Prostate Specific Antigen (PSA) detection at low concentrations, Fang et al. [53] presented a signal amplification method using QDs-aptamer/GO FRET system and DNase I enzyme. In this assay, the QD-aptamer molecules adsorbed onto a GO sheet through π -interactions and were released, due to the sensitive binding of PSA with

the QD-aptamer hybrid. This release was followed by breaking off the oligonucleotide structure of the aptamer by DNase I addition. Hence, the QDs and PSA molecules were liberated, and PSA can again bind to a new QD-aptamer hybrid in a new cycle. Consequently, the fluorescence signal related to QDs was amplified, and PSA quantification sensitivity in human serum was significantly improved. In another assay [58], a paper-based heterogeneous method was proposed for detection of the Epithelial Cell Adhesion Molecule (EpCAM) by an aptamer-functionalized QDs on a modified cellulose paper. The aptamer was hybridized with Cy3-labeled complementary DNA (cDNA). In close proximity to the QD surface, FRET emission of Cy3 dye occurred; however, competitive binding of the target biomarker to the aptamer was followed by a decrease in the FRET efficiency, due to the displacement of the cDNA. This solid-phase assay improved the LoD compared to the solution-phase FRET variant. Aflatoxins, on the other hand, are the most common group of toxins that lead to food product contamination and are secondary metabolites produced by *Aspergillus* species [12]. Because aflatoxin B1 is known to be highly toxic, Sabet et al. [59] developed a FRET-based biosensor for rapid aflatoxin B1 detection, by using QDs as the energy donor and AuNPs as the energy acceptor molecule. The absorption spectrum of the QDs overlapped well with the emission spectrum of the AuNPs. Without aflatoxin B1, the aptamer-QDs conjugate was brought near the AuNPs, due to the interaction of aptamers with AuNPs leading to quenched emission on QDs fluorescence. In the presence of Aflatoxin B1, the aptamer breaks the interaction with AuNPs, thus, restoring fluorescence. The

method resulted in a dynamic range between 10 and 400 nM, with a detection limit of 3.4 nM. Equally important that the same linear range was obtained in rice and peanut samples, indicating high robustness of the developed nanoprobe. In Table 1, selected examples from the recent literature are summarized for QD and aptamer-based FRET assays.

Although QDs are commonly utilized as the donor species in FRET pairs, they can also be used as acceptors, due to their high absorption coefficients and characteristic absorption spectra [13]. This concept was applied first by Hildebrandt et al. using lanthanide complexes as donors [60], and shortly afterward by So et al., who used bioluminescent donor molecules along with QDs as the acceptor [61]. Many other assays have been developed with QDs as the acceptor molecules and different donor molecules, such as lanthanide complexes, upconverting nanoparticles, QDs, dyes, or bio/chemiluminescent molecules that are extensively reviewed elsewhere [13]. In many of these FRET assays, DNA, or

RNA hybridization strategy are used for biological recognition [1, 62–66]. Only a single study was performed with aptamer modified QD as acceptors. Doughan et al. demonstrated a distinct thrombin aptamer-based sandwich assay with immobilized NYF₄:Yb³⁺, Tm³⁺/β-NaYF₄ core/shell UCNPs as the donor and CdS_xSe_{1-x}/ZnS core/shell QDs as the acceptor nanoparticles [67]. In this FRET-based system, UV and blue emissions of Tm-doped UCNPs around 340–370 nm and 440–490 nm bands were used; the donor emission and energy transfer of these excited states led to emission from donor QDs at wavelength of 614 nm, as both aptamers were bound on the thrombin analyte leading to thrombin detection at concentrations as low as 0.1 μM.

In retrospect, QDs stand out as almost ideal FRET donor, due to their high quantum yields, broad excitation profiles, and considerably sharp emission profiles. Although photoexcitation across their band gap enables the excitation of multiple QDs with a spectrum of different emissions, it severely

Table 1 Aptamer-based FRET assays utilizing QDs as donor/acceptor molecules. Respective aptamer sequences and the calculated limit of detection (LoD) values were also presented

Signal	Donor	Acceptor	Target	Aptamer	LoD	Ref.
On	QDs	AuNPs	Bisphenol A	CCGGTGGGTGGTCAGGTGGGATAGCGTTCGCGTATGG CCCAGCGCATCACGGGTTCCGACCA	1.86 ng/mL	[68]
–	QDs	AuNPs	Mercury (II)	TTTTTTTTT	2.5 pM	[69]
Off	QDs	Cy3 dye	EpCAM	AGCGTCAATACCACTACAGTTGGCTCTGGGGGATGT GGAGGGGGTATGGGTGGGAGT CTAATGGAGCTCGT GGTCAG	250 pM	[58]
On	QDs	AuNPs	Aflatoxin B1	GTTGGGCACGTGTTGTCTCTGTGTCTCGTGCCCTTC GCTAGGCC	20 pg/mL	[70]
–	QDs	GO	Aflatoxin B1 (toxin)	ATATCTTTTCTACTCATCTTTGAATAACTACGGGCA TTACTTTCTGGCCTCCCTGCCTCCTAAATACCAAT TAATTCGGCGCCCCCG	0.004 mg/mL	[12]
Off	QDs	AuNPs	PSA	ATTAAGCTCGCCATCAAATAGC	1 Pg/mL	[71]
On	QDs	MoS ₂	Ochratoxin A (toxin)	CCTGGGAGGGAGGGAGGGATCGGGTGTGGGTGGCGTAA AGGGAG-CATCGGACACCCGATCCC	1.0 ng/mL	[72]
On	QDs	Hemin/G-quadruplex DNase	Lysozyme	ATCAGGGCTAAAGAGTGCAGAGTTACTTAG	2.6 nM	[73]
On	QDs	AuNPs	Aflatoxin B1 (toxin)	GTTGGGCACGTGTTGTCTCTGTGTCTCGTGCCCTTC GCTAGGCCACA	3.4 nM	[59]
On	QDs	GO	PSA (biomarker)	TTTTTAATTAAGCTCGCCATCAAATAGCTTT	0.05 fg/mL	[53]
On	QDs	GO	Aflatoxin B1 (mycotoxin)	TCGTCCATGTGTTGGGCACGTGTTGTCTCTGTGTCT CGTGCCCTTCGTAGGCCACACGATGCGTAG	1.0 nM	[74]
Off	QDs	Aptamer-modified Cy5.5	Acetamiprid	CTGAC ACCATATTAT GAAGA	0.02 mM	[75]
Off	QDs	CNPs	<i>Vibrio parahaemolyticus</i>	ATAGGAGTCACGACGACCAGAATCTAAAAATGGGCAAA GAAACAGTGACTCGTTGAGATACTTATGTGCGTCTA CCTCTTGACTAAT	25 cfu/mL	[57]
Off	QDs	CNPs	<i>Salmonella typhimurium</i> (pathogen)	ATAGGAGTCACGACGACCAGAAAGTAATGCCCGTAGT TATTCAAAGATGAGTAGGAAAAGATATGTGCGTCTA CCTCTTGACTAAT	35 cfu/mL	[57]
–	QDs	AuNPs	17β-Estradiol	GCTTCCAGCTTATTGAATTACAGCAGAGGGTAGCGGC TCTGCGCATCAATTGCTGCGCGCTGAAGCGCGAAGC	0.057 ng/mL	[76]
On	UCNP	QDs	Thrombin	AGTCCGTGGTAGGGCAGGTTGGGGTGGTACT GGTTGGTGGTTGG	0.1 μM	[67]

limits their multiplex potential as active (emissive) FRET acceptors. Broad excitation profiles lead to unwanted excitation of QD acceptors when they were intended for accepting the excited states of donor species. In this context, QD donors are paired with active acceptors that have narrow excitation profiles, such as fluorophores. On the other hand, FRET pairs for QD donors and plasmonic nanostructure-based passive (non-emissive) acceptors have seen considerable attention, due to complimentary excitation/absorption profiles. However, these studies were stayed restricted to the spherical gold nanoparticles. The plethora of plasmonic nanostructures that can absorb specific portions of the visible to NIR should be explored to exploit the size-tunable QD donors with high quantum yield.

Upconverting Nanoparticles (UCNPs)

UCNPs are attractive FRET donors, due to their relatively long lifetime, better biocompatibility compared to heavy metal containing QDs [77], and low excitation energy in NIR. UCNPs are lanthanide-doped nanomaterials that absorb two or more low energy photons and emit a high-energy photon through electronic transitions in the dopant structure [78]. Hence, depending on the dopant/host combination, UCNPs can emit light from NIR to UV [79]. Since the electron relaxation time of UCNPs is in the μs time frame, UCNP-based FRET systems are often referred to as luminescence resonance energy transfer (LRET) in the literature [80]. With the anti-Stokes shift in their electronic structure, UCNPs can emit high-energy luminescence in the near-field stimulated by low-energy excitation, such as by those in the NIR. As a result, UCNPs enhance the signal-to-background noise ratio of these platforms by minimizing the luminescence from surrounding molecules [42]. This property of UCNPs makes them ideal candidates for detection of biological samples, where the stimulus required to excite the donor must be out of the absorption range of the surrounding environment. In addition to the anti-Stokes shift, doping with rare-earth ions also provides a long luminescence lifetime to UCNPs.

With regard to the lanthanide group components, outer shell $5s^2 5p^6$ electrons provides screening for the electrons in partially or filled 4f orbitals. Accordingly, f-f transitions become unlikely, which prolongs the luminescence lifetime [81]. FRET rate is inversely proportional to donor lifetime (Eq. 1), and long lifetimes are thus less favorable for high FRET rates. Commonly used donors for FRET assays are Yb^{3+} and Er^{3+} doped NaYF_4 UCNPs, which have excitation energy in the NIR region [82]. This property becomes very important for cases, in which deep tissue signal detection is needed. NIR excitation of UCNPs enables them to penetrate deep tissue without harming biological samples, in contrast to UV excitation. This unique advantage has made UCNPs excellent candidates for in vivo tumor-imaging, when coupled with gold nanorods (AuNRs) [80].

UCNPs are also coupled with other well-known radiative quenchers like GO and even organic dyes for a wide range of applications; in which they are used to trace molecules such as DNA [83], mRNA [84], antigens [45], virus [85], pesticides [86], antibiotics [87] and bacteria [88]. Regarding PSA detection, Hao et al. [89] reported a self-assembled pyramid structure of Au-UCNPs. The AuNPs quenched the luminescence of UCNPs, and aptamer-functionalization resulted in PSA detection with attomolar sensitivity. The quenched fluorescence of the UCNPs was recovered as the UCNPs were released from the pyramid structure while binding to the target through the coupled aptamers. For ultra-sensitive detection of Alphafeto protein (AFP), a self-assembled Au-Au-UCNP nanoprobe was designed using conjugated oligonucleotides [90]. Binding of AFP with an AFP-specific aptamer conjugated to the UCNPs led to blockage of resonant energy transfer from the UCNPs to AuNPs. Increasing concentration of AFP resulted in the recovery of UCNP fluorescence intensity, and the detection limit was again found in attomolar range (0.059 aM). This approach stands out among others, due to the broad linear range and lowest LoD achieved. In another example, a different strategy was reported for the detection of CEA utilizing $\text{NaYF}_4: \text{Yb}^{3+}, \text{Er}^{3+}$ UCNPs, and AuNPs as the energy donor and acceptor molecules, respectively [45]. UCNPs have excellent prospects as candidate energy donors for FRET-based biosensors. AuNPs as well-organized quenchers with broad absorption spectrum were selected as the energy acceptors of UCNPs. The low limit of detection related to this analysis was around 0.02 ng/mL. This biosensor was applicable for CEA protein detection because of features including great selectivity and reproducibility.

In the detection study of *E. coli* ATCC 873 by Jin et al. [42], AuNPs were coupled with the target-selective aptamer and UCNPs were functionalized with the cDNA molecules. The authors obtained the quenching of the UCNP luminescence through the attraction between the aptamer and the complementary sequence. However, in the presence of the *E. coli* ATCC 873, the aptamer-AuNPs desorbed and became bound to the target, which resulted in the recovery of initial green fluorescent signals, as shown in Fig. 4 [42]. Desorption occurred via the affinity of the aptamer and the high mobility of the FRET probe, compared to the larger analytes. The aptamer used for Hg^{2+} ion detection, on the other hand, folds into the hairpin structure in the presence of the target ion, as mentioned previously. The reason that the aptamer adopts the hairpin structure is the stable bond that occurs in between thymine residues and Hg^{2+} is even more stable than the adenine-thymine bound [98]. Likewise, Liu et al. [92] used aptamer-modified UCNPs as donors and AuNPs as the acceptors for Hg^{2+} -selective FRET-based UCNP approach. In this study, the Hg^{2+} selective aptamer sequence was 5' $\text{NH}_2\text{-C}_6\text{-CTACAGTTTCACCTTTTCCCCCGTTTTGGTGTTC-3'}$, and the complementary ssDNA was 5' $\text{SH-C}_6\text{-GAAACTGTAG-3'}$. Not surprisingly, the selective aptamer contained multiple thymine residues,

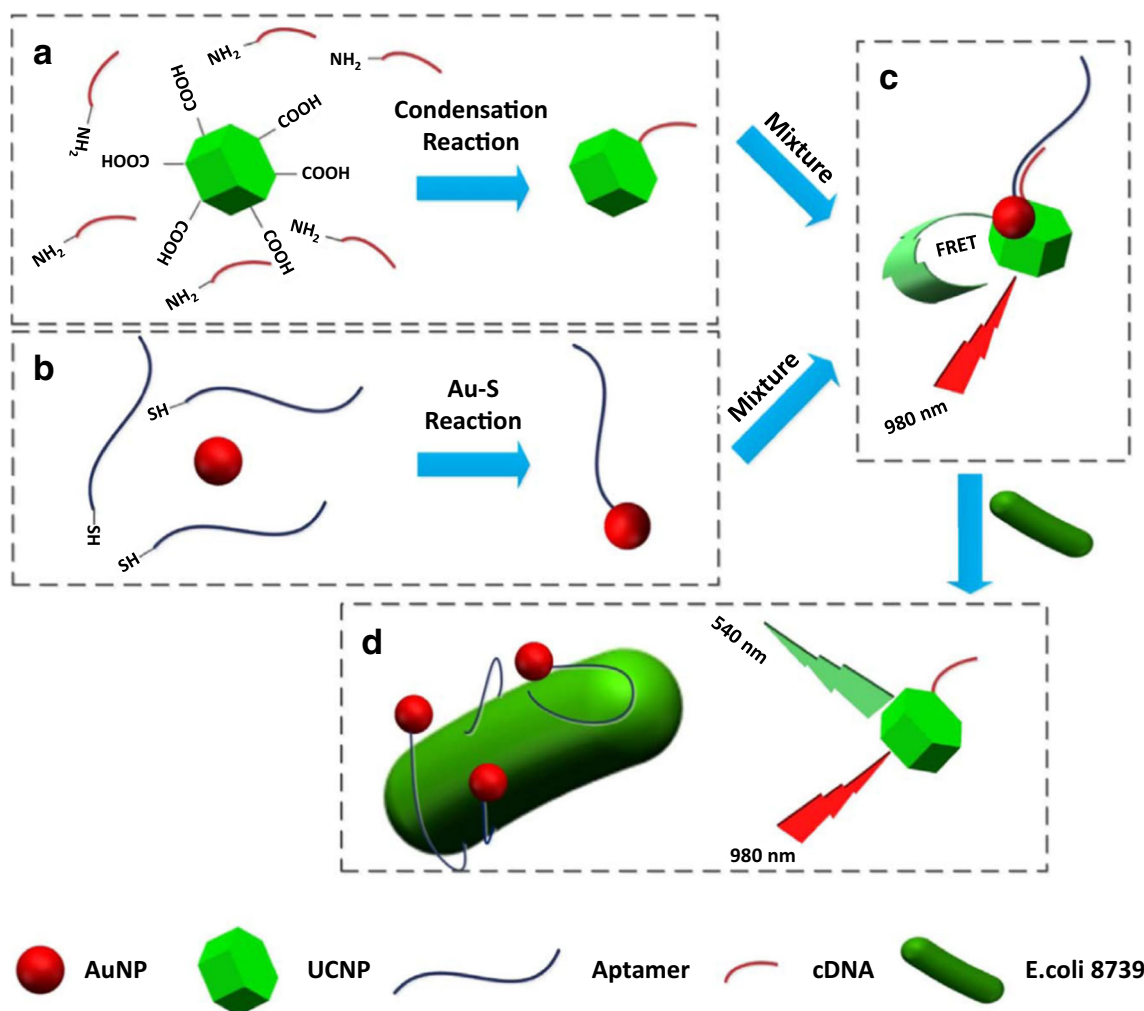


Fig. 4 Schematic illustration of UCNP-based FRET aptasensor for bacteria detection; (a) NH_2 -labeled cDNA of the aptamer is coupled to COOH-labeled UCNPs by condensation reaction; (b) Conjugation between thiolated aptamers and AuNPs through deprotonation; (c)

Formation of FRET pair (UCNPs-cDNA and AuNPs-aptamer) through complementary bases; d) Recovery of the green fluorescent signal in the presence of target bacteria. Adapted from [42]

whereas the complementary strand had none to allow hairpin formation. A couple of examples, in which the aptamer modified UCNPs were used as the donor molecules in FRET assays, are summarized in Table 2.

Even though UCNPs inherently offer extremely sharp emission peaks for biosensing applications, their quantum efficiencies are significantly lower (below 2%) than QDs and fluorophores. Because anti-Stokes type emission from UCNPs depends on the time-dependent population of excited Yb^{+3} state, rate-limited successive excitation of excited Yb^{+3} , and the internal energy transfer between Yb^{+3} to the emission ion (e.g., Er^{+3} , Tm^{+3}), the rate limited UCNP emission eventually results in excitation power density-dependent quantum yield profile. Thus, the use of high-power excitation lasers with a wavelength of ca. 980 nm (${}^2\text{F}_{7/2} \rightarrow {}^2\text{F}_{5/2}$ transition of Yb^{+3}) is widespread in UCNP based FRET assays. Unfortunately, an excitation wavelength of 980 nm also coincides with a broader vibrational absorption of water ($\nu_1 +$

ν_2 , 970 nm, 10310 cm^{-1}) [99]. The vibrational absorption of water leads to rapid elevation of temperature in the assay and jeopardizes the efficacy and reliability of the UCNP FRET assays. In order to remedy this, Nd^{+3} is utilized as an alternative sensitizer instead of Yb^{+3} and effectively switched the preferred excitation wavelength to 800 nm. However, the low quantum yield remains a prominent issue.

Graphene Quantum Dots (GQDs) and Carbon Dots (CDs)

Carbon-based photoluminescence materials, like GQDs and CDs, are alternatives to QDs that usually contains heavy metals. GQDs, which are graphene flakes smaller than 20 nm [100], serve as donors in FRET studies due to their good solubility, ease of synthesis [101] and modification capabilities [102]. Moreover, GQDs display quantum confinement effects as a result of their small and tunable size, which

Table 2 Aptamer-based FRET methods utilizing UCNPs as the donor molecules. Respective aptamer sequences and the calculated LoD values are presented

Signal	Donor	Acceptor	Target	Aptamer	LoD	Ref.
On	UCNPs	Au-NPs	CEA	ATACCAGCTTATTCAATT	0.02 ng/mL	[45]
On	UCNPs	SYBR Green I	Oxytetracycline	GGAATTCGCTAGCACGTTGACGCTGGTGCCCGGTTGTGGTGCGA GTGTTGTGTGGATCCGAGCTCCACGTG	0.054 ng/mL	[91]
On	UCNP	AuNPs	Mercury	CTACAGTTTCACCTTTTCCCCCGTTTTGGTGT	60 nM	[92]
Off-On	UCNPs	GO	CEA	ATACCAGCTTATTCAATT	10.7 pg/mL	[93]
Off	UCNPs	AuNPs	<i>E. coli</i> ATCC 873	GCAATGGTACGGTACTTCCCCATGAGTGTGTGAAATGTT GGGACACTAGGTGGCATAGAGCCGCAAAGTGCACGCT ACTTTGCTAA	5–10 ⁶ cfu/mL	[42]
On	UCNPs	BHQ1 BHQ3	Microcystin-LR	GGCGCCAAACAGGACCACCATGACAATTACCCATACCACCTCAT TATGCCCCATCTCCGC	0.1–50 ng/mL	[94]
On	UCNPs	BHQ1 BHQ3	Okadaic acid	GGTACCAACAACAGGGAGCGCTACGCGAAGGGTCAATGTGA CGTCATGCGGATGTGTGG	0.1–50 ng/mL	[94]
–	UCNPs	AuNPs	PAT	GGCCCGCCAACCCGCATCATCTACACTGATATTTACCTT	0.003 ng/mL	[95]
On	UCNPs	AuNRs	<i>S. typhimurium</i>	GCAATGGTACGGTACTTCTCGGC ACGTTTCAGTAGCGCTCGCT GGTCATCCACAGCTACGTCAAAGTGCACGCT ACTTTGCTAA	11 cfu/mL	[88]
On	UCNPs	AuNPs	Acetamiprid	CTGACACCATATTATGAAGA	3.2 nM	[77]
Off	UCNPs	Palladium nanoparticle	CEA	ATACCAGCTTATTCAATT	1.7 pg/mL	[96]
–	UCNPs	AuNPs	AFP	GGCAGGAAGACAAACAGGACCGGGTTGTGTGGGGTTTAAGAGC GTCGCCTGTGTGTGGTCTGTGGTGCTGT	0.059 aM	[90]
On	UCNPs	AuNPs	PSA	TTTTTAATTAAGCTCGCCATCAAATAGCTTT	0.032 aM	[89]
On	UCNPs	AuNRs	Ochratoxin A	GATCGGGTGTGGGTGGCGTAAAGG GAGCATCGGACA	27 Pg/mL	[97]

allows tailoring their excitation energy spectrum, specifically between 300 and 470 nm [103]. Using GQDs as donor molecules in FRET systems enables excitation of the system beyond the excitation range of the acceptor, resulting in enhanced luminescence signals [104]. The most significant drawback of GQDs is their low luminescence quantum yield that is around 28% [105].

With the aim of EpCAM detection, a “turn-on” fluorescence biosensor based on the use of GQDs and molybdenum disulfide (MoS₂) nanosheets was proposed by Shi et al. [106]. In their work, PEGylated GQDs were labeled with the EpCAM-specific aptamer adsorbed on MoS₂ surface via Van der Waals forces. Following FRET between GQD and MoS₂ in the presence of EpCAM, the interaction between the aptamer and EpCAM protein led to the detachment of the GQD-labeled EpCAM aptamer from MoS₂ nanosheets. The LoD for this detection method was in the picomolar range.

Small molecule toxins that aptamers have been selected for their detection can be divided into three groups: mycotoxins, cyanotoxins, and toxins from dinoflagellates [107]. Ochratoxin (OTA), for example, is a prevalent mycotoxin that is a continual impurity of foods such as coffee. It has immunotoxic and carcinogenic effects in humans and animals [108, 109]. In grains, an acceptable level for OTA has been set by commissions; hence, it is crucial to provide one efficient method for detection of OTA. In a recently published report [110], biosensors for OTA based on FRET mechanism from

nanoceria to GQD were shown to have a low detection limit in the picomolar range. FRET between nanoceria and GQDs took place efficiently because the emission spectrum of the nanoceria partially covered the absorption spectrum of GQDs.

CDs, on the other hand, are carbon particles with diameters smaller than 10 nm. They have all the advantages of GQDs, like resistance to photo-bleaching, and spectral tunability of emission spectrum arising from the quantum confinement effect [111, 112]. Moreover, they have low toxicity, even lower than the heavy metal-free semiconductor QDs [113]. However, poor repeatability of synthesis leads to batch-to-batch variation in size, structure, emission wavelength and quantum yield. With these significant drawbacks, carbon-based nanomaterials are poor donor candidates for FRET-based detection assays [114].

In one example [115], quantitative detection of Adenosine (AD) was achieved through aptamer-modified CDs-based FRET assay where FRET occurred between nano-graphite (acceptor) and aptamer modified CDs (energy donor). In the existence of AD, FRET was blocked by the interaction between AD and its aptamer. Fluorescence of the aptamer-modified CDs was recovered through dissociation of CDs-aptamer from the nano-graphite surface. As several methods using CDs as luminescent probes operate in the turn-off mode, they are less sensitive to strong matrix effects. On the other hand, CDs FRET nanoprobe can also function on the turn-on principle [115, 116]. In Table 3, several examples are summarized where the

Table 3 FRET assays utilizing CDs and QDs as the donor molecules, respective aptamer sequences, and the calculated LOD values

Signal	Donor	Acceptor	Target	Aptamer	LoD	Ref.
On	GQDs	Graphene oxide	Lead (II)	GGGTGGGTGGGTGGGT	0.6 nM	[117]
On	GQDs	MoS ₂	EpCAM	CACTACAGAGGTTGCGTCTGTCCCACGTTGTC ATGGGGGGTTGGCCTG	450 pM	[106]
Off	CDs	AuNPs-PAMAM Dendrimer/aptamer	CA 15–3 tumor marker	GAAGTGAATATGACAGATCACAACCT	0.9 μU/mL	[113]
Off	CDs	Graphene oxide	ATP	ACCTGGGGGAGTATTGCGGAG GAAGGT	80 pM	[111]
On	CDs	Nano-graphite	Adenosine	ACCTGGGGGAGTATTGCGGAGGAAGGT	0.63 nM	[115]
Off	CDs	Cobalt oxyhydroxide nanosheets	Methamphetamine	ACGGTTGCAAGTGGGACTCTGGTAGG CTGGGTAAATTTGG	1 nM	[118]
On	CDs	AuNPs	Adenosine	AGAGAACCTGGGGGAGTATTGCGGAG GAAGGT	4.2 nM	[119]
On	CDs	AuNPs	ATP	ACCTGGGGGAGTATTGCGGAGGAAGGT	8.5 nM	[120]
On	CDs	Nano-graphite	Dopamine	GTCTCTGTGTGCGCCAGAGAACA CTG GGGCAGATATGGGCCAGCACAGAA TGAGGCC	0.055 nM	[121]
On	CDs	AuNPs	AFB1	AAAAAAGTTGGGCACGTGTGTCTCT CTGTGTCTCGTGCCTTCGCTAGGCCCA CA	5 pg/mL	[122]
On	CDs	AuNPs	Hg ²⁺	TTCTTTGTTCCCTTCTTTGTT AACAAAGAACCCCCCCCC	0.7 pM	[11]
On-Off-On	CDs	MoS ₂	Kanamycin (Antibiotic)	TGGGGGTTGAGGCTAAGCCGA	1.1 μM	[123]

analytes are mostly small molecules (such as disease biomarkers, antibiotics, and heavy metals) and the calculated LoDs var. from picomolar sensitivity to micromolar range.

Metal-Organic Frameworks (MOFs)

MOF structure consists of an organic 3D network cage surrounding a metal atom, which allows the generation of versatile structures by changing metal cores or caging organic network for various applications. This unique structure of MOFs gives rise to a high level of functionality, noticeable thermal and mechanical stability, large pore sizes due to metal composition organic linkers (or metal clusters, chains, or layers), and substantial surface area [124]. MOFs have been extensively used in applications, such as catalysis, drug delivery [125], and small molecule detection [126]. It is worth mentioning that the variable chemical composition of MOFs leads to the toxicologically acceptable formulations. Depending on the selected metal, MOFs can function as either donor or acceptor, and the subject is still a contentious one in the community. With their mutable roles and porous organic network, all MOFs provide a high density of surface area that enables target modification and adsorption. MOFs like Cd-MOF [109] and Tb-MOF [127] are examples of donors, while Cu-MOFs have served as acceptors [43] in FRET-based assays.

Graphene, Graphene Oxide (GO) and Reduced Graphene Oxide (rGO)

Graphene, GO, and rGO are accepted as universal quenchers, and they have been used as acceptor surfaces in many energy transfer-based applications [128]. Highly efficient photoinduced electron transfer ability of graphene materials due to their unique large conjugated structure provides a broad absorption spectrum [14], which makes possible to couple graphene materials with various energy donors such as Au NCCDs [111], QDs [129] and UCNPs [84]. FRET-based detection systems mostly work in liquid phases like buffers, human serum, or whole blood [130]. With their ease of synthesis and good water solubilities, graphene materials are very suitable for quick one-pot applications [56] and paper-based biosensing through inkjet printing [131]. They readily adsorb single-stranded (ss) nucleic acids like mRNA and ssDNA through their π -interactions, whereas double chained nucleic acids are avoided [87]. This particular property of graphene has been tested by Alonso-Cristobal et al. [132] to define the sufficient concentration of acceptor molecules in order to quench the emission of the donor for UCNP-based DNA detection FRET assay.

Adsorption can also be achieved directly by chemical interactions between aptamers and the FRET probes; moreover, its strength can be adjusted to favor the desorption in the presence of the analyte. This situation was demonstrated by Furukawa et al. [133], where the authors employed an aptamer selective to PSA and compared the detection limit when the aptamer was coupled with graphene and GO. Aptamers make

π -stacking through their organic nitrogenous bases with both graphene and GO, whereas they additionally bound with GO through the hydrogen bonding that located at both backbones of aptamer and terminus hydrogens of the nitrogen bases. Hence, the desorption of aptamers from GO is more complicated than graphene, which leads to having a higher limit of detection when the same aptamer is coupled with GO.

Although several graphene-based materials show similar properties in a structural manner, they still have chemical and physical differences resulting from the synthesis methodology. GO is commonly synthesized by Hummers' method, which contains chemical oxidation of graphite molecules. Consequently, GO flakes bear oxygen-containing groups like hydroxyl and carboxyl, unlike pristine graphene. The presence of hydroxyl groups on the surface provides an additional site that enables the adsorption of affinity molecules without the help of π -interactions [134]. Signal-on detection of small molecules with FRET principle is only possible with the structural change of the aptamer since the mobility of the target is higher than the aptamer, desorption can only happen due to a structural configuration change. Detection of ATP can be an excellent example of a small biological molecule with aptamers and GO. As recently reported by Cheng et al. [111], ATP selective aptamer folds through its organic nitrogenous groups and creates a globular chain structure in the presence of ATP. As a result of that, side groups can contribute to hydrogen bonding, and π -interactions on aptamer gets blocked and release the aptamers from the GO surface, which was used as the acceptor molecule in the report.

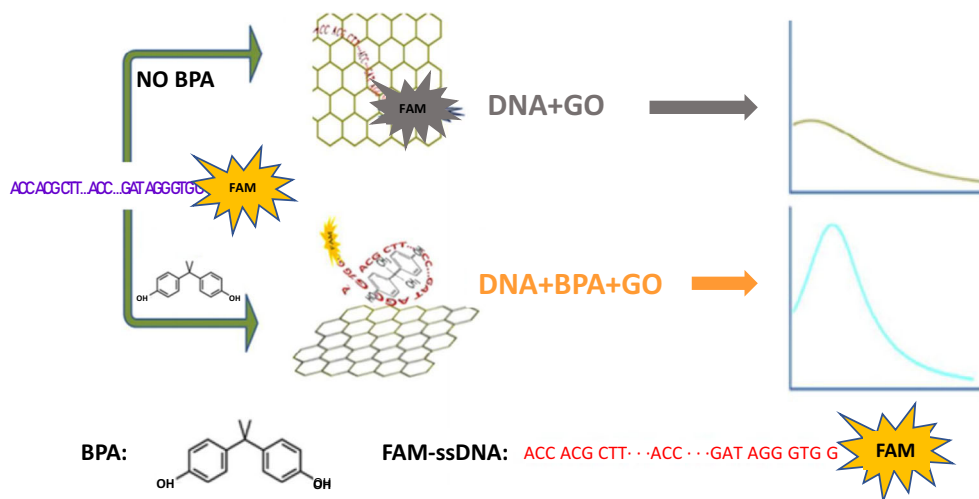
Mass spectrometry stands out among the other conventional methods for detection of small chemical molecules. In stark contrast, using this technology correctly requires large equipment along with a high degree of training at a cost. Although the aptamer-based assays may not provide that are as accurate results as mass spectrometry, they can still be used with little training for on-site measurements. Food and drinking water are firmly checked to prevent their contamination by hazardous substances or microorganisms. In order to improve this routine control, detection of contaminants and their removal is of great importance. Following this, one of the most popular targets for aptamer detection is Bisphenol A (BPA), which is used in the production processes of food-storage components and plastics. It is now regarded as an environmental pollutant which is hazardous to human and animal health and has been reported to be toxic [135, 136]. For selective detection of Bisphenol A, a method was designed by Zhu and his co-workers [137] based on GO and an anti-BPA aptamer. GO was used to quench fluorescently labeled ssDNA probes in its free form but not the folded form after target binding. BPA can be coupled with anti-BPA aptamer and alter its structure to prevent the aptamer from adsorbing onto the surface of GO. LoD found out to be 0.05 ng/mL, and the developed method was strongly applicable to actual water samples as represented in Fig. 5 [137].

Heavy metal ions are another area of application that FRET can be used since ions are small and exist in trace amounts in most of the subjects. As demonstrated by Qian et al. [117], GO flakes quenched the signal from the aptamer-labeled QDs in the absence of Pb^{2+} . When ions were introduced into the sample, the aptamers immediately formed a G-quadruplex conformation and surrounded Pb^{2+} ions. Aromatic nucleobases in the G-quadruplex structure that provided the π -stacking with GO was blocked by phosphate groups which weakened the interaction of donor and acceptor and generated the final signal. Since shielded π -stacks achieved desorption, acceptor material must be carefully chosen as sp^2 -hybridised material to obtain accuracy and high sensitivity.

Despite their large surface area and unique physicochemical properties, graphene materials have a significant drawback of low recovery of the incident fluorescence signal, which indicates the low desorption of the fluorescent materials caused by relatively strong π -interactions and hydrogen bonds in case of GO and rGO. rGO, on the other hand, has structural damages or defects on the surface as a result of the chemical reduction of GO flakes. These defects on rGO act as electron traps that improve the adsorption of the molecules to the surface. However, due to the reduction step in the synthesis of rGO, the number of oxyl-groups decreases, which cause a weaker adsorption capability to the material, as compared to the other graphene species [138]. Zhou et al. [139] stated in their FRET study for Carcino-embryonic antigen (CEA) detection that fluorescence quenching efficiency was extremely strong even in aptamer free QDs and jeopardizing the detection of the intended analyte. To keep the FRET as a versatile detection technique, fluorescence recovery issues need to be solved, and more sophisticated techniques should be developed for challenging applications like miRNA detection in living cells where aptamers are used to construct 3D structures with nanomaterials such as a molecular beacon, nanopyramids, and nanotweezers. Recently, researchers have utilized Transition Metal Dichalcogenides nanosheets (TMD-NSs), such as MoS_2 , TiS_2 , TaS_2 , and WS_2 as potential energy acceptor molecules [140]. Unlike graphene materials, TMD-NSs adsorb single-stranded nucleic acids on their surface via weak Van der Waals interactions [141]. Hence, higher fluorescent signal recoveries are achieved as compared to the graphene materials [123].

Yuan et al. [142] employed WS_2 for DNA detection, Zhang et al. [143] used MoS_2 , TiS_2 , and TaS_2 , and for FRET assays and finally, Ge et al. [144] employed MoS_2 for ATP detection with a low LoD as compared to graphene material-based FRET assays. In the report by Cui et al. [145], a magnetic fluorescent biosensor based on GQDs, Fe_3O_4 , and MoS_2 nanosheets were designed for selective detection of circulating tumor cells (CTCs). This "turn-on" biosensing magnetic fluorescent nanocomposite (MFNs) consisted of MoS_2 nanosheets as the fluorescence quencher and aptamer@ Fe_3O_4 @GQD

Fig. 5 Schematic demonstration of GO-based FRET assays; (a) cocaine detection by the label-free fluorescent aptamer-based assay using GO and isothermal circular strand-displacement amplification method [48]; (b) Bisphenol A (BPA) detection using a FRET-based aptasensor [137]



assembly as the donor molecule. In comparison with other one-step and two-step marker detection methods, MFNs were capable of labeling the target CTCs within 15 min. Another striking feature of MFNs is being able to capture CTCs due to the existence of aptamers [145]. Gao et al. [146] proposed a FRET-based assay using MoS₂-aptamer nanosheets for thrombin detection. In this assay, MoS₂ and exonuclease co-assisted signal amplification strategy were applied to enhance the detection limit of thrombin up to femtomolar sensitivity. As can be seen from Table 4, this type of FRET methods was mostly designed in signal-on fashion, and the analytes varied from large bacterium cells to small molecules like ATP and Bisphenol A.

Two-dimensional materials provide a suitable acceptor candidate for aptamer-based FRET assays in theory. However, the strong affinity of these 2D acceptors also introduce complications such as strong binding of aptamer species on these surfaces and limited fluorescence/luminescence recovery. Especially, non-specific binding of analyte and detection probes on graphene and its derivatives emerges as a significant concern. As an example, strong quenching efficiency of graphene derivatives resulted in low fluorescence/luminescence recovery rates even when non-functionalized fluorescent species introduced into the solution [37, 139]. In order to reach up to the full potential of 2D materials, issues of strong quenching efficiency of graphene derivatives and non-specific interactions have to be addressed in the future.

Gold Nanoparticles (AuNPs)

Metal nanoparticles (MNPs) can exhibit an energy transfer mechanism based on the non-radiative energy transfer between excited donor state and Fermi level of the metal surface. This phenomenon is defined as nanometal/nano surface energy transfer (NSET) [158]. Although NSET also requires energetic resonance (spectral overlap), energy is transferred from a

point-dipole to a surface in FRET (many point-dipoles on a surface) instead of point-dipole to point-dipole. Therefore, the rate of energy transfer is proportional to R^{-4} , unlike R^{-6} in FRET [3, 159]. This R^{-4} distance dependency can double the effective interaction between donor and acceptor molecules. NSET distance, R_0^{NSET} , is calculated as [160]:

$$R_0^{NSET} = \left[0.225 \frac{c^3 \Phi_D}{\omega_D^2 \omega_F k_F} \right]^{\frac{1}{4}} \quad (5)$$

where Φ_D is the quantum yield of the donor, c is the speed of light, ω_D is the angular frequency of the donor, ω_F is the angular frequency of bulk gold, and k_F is the Fermi vector for bulk gold. The resulting quenching efficiency of nano-metal surface energy transfer, E_{NSET} , is shown as.

$$E_{NSET} = 1 - \frac{1}{1 + \left(\frac{R_0^{NSET}}{R} \right)^4} \quad (6)$$

where R is the distance of donor from the metal surface.

MNPs have been used as an energy acceptor for various analytical applications ranging from virus detection [85] to metal ion detection [92]. Due to their biocompatibility and broad absorption spectrum, AuNPs are arguably the most utilized material as acceptors in energy transfer-based biosensors, and most studies use the term FRET instead of NSET for describing the energy transfer. AuNPs exhibits localized surface plasmon resonance (LSPR) behavior coinciding with the visible spectrum. This phenomenon originates from the collective oscillations of free electrons in the metal surface.

The limited surface of a single nanoparticle results in insufficient decay of the surface-bound plasmons and leads to well-defined modes of surface plasmons called localized surface plasmon resonance. This phenomenon was employed to trace GA for diabetes diagnosis by Ghosh et al. [39], as shown in Fig. 6 [39]. In the study, CdSe/ZnS QD was chosen as the

Table 4 Recent FRET methods utilizing Graphene, GO and MoS₂ as the FRET acceptors

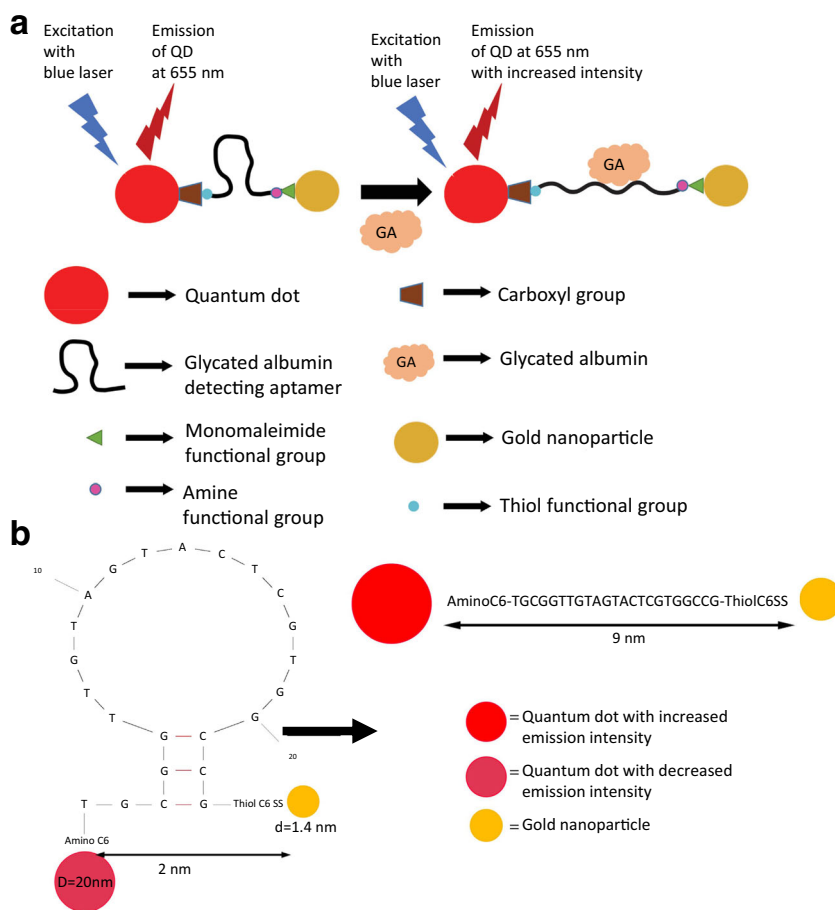
Signal	Acceptor	Donor	Target	Aptamer	LoD	Ref.
On	GO	FAM labelled aptamer	Bisphenol A	CCGGTGGGTGGTCAGGTGGGATAGCG TTCCGCGTATGGCCCAGCGCATCA CGGGTTCGCACCA	0.05 ng/mL	[137]
On	MoS ₂	GQD	CTCs	CACTACAGAGGTTGCGTCTGTCCCACGTTGTC ATGGGGGGTTGGCCTG	1.19 nM	[145]
On	Graphene and GO	FAM labelled aptamer	PSA	TTTAATTAAGCTCTCCATCAAATAGC	>500 ng/mL	[46]
On	MoS ₂	FAM labelled aptamer	Plasmodium lactose dehydrogenase	GTTTCGATTGGATTGTGCCGGAAGTGC TGGCTCGAAC	550 pM	[140]
On	MoS ₂	FAM labelled aptamer	Salmonella typhimurium	ATAGGAGTCACGACGACCAGAAAAGTA ATGCCCGGTAGTTATTCAAAGATGAGTAGG AAAAGATATGTGCGTCTACCTCTTGACTAAT	10 cfu/mL	[141]
On	MoS ₂	Chlorine e6 labelled ATP aptamer	Intracellular ATP	AACCTGGGGGAGTATTGCGGAGGAAGGT	5 μM to 3 mM	[147]
On	MoS ₂	FAM labelled aptamer	Thrombin	AAAAGTCCGTG GTAGGGCAGGTTGG GGTGACT	6 fM	[146]
On	MoS ₂	FAM labelled aptamer	Arsenic ions	GTAATACGACTCACTATAGGGAGATACCAGCT TATTC AATTTTACAGAAACAACCAACGTCGC TCCGGTACTTCTTCATCGAGATAGTAAAGT GCAATCT	18 nM	[148]
On	MoS ₂	Aptamer induced multicolored AuNCs	AFP	GGCAGGAAGACAAACAAGCTTGGCGG CGGGAAGGTGTTAAATTCGCGGTCTGCG TGGTCTGTGGTGCTGT	0.16 ng/mL	[149]
On	MoS ₂	Multicolored AuNCs	CEA	ATACCAGCTTATTCAATT	0.21 ng/mL	[149]
On	MoS ₂	QDs	Dopamine	GTCTCTGTGTGCCAGAGAACACTG GGCAGATATGGGCCAGCA CAGAATGA GGCC	45 pM	[150]
Off-On	rGO	FAM labelled aptamer	Ricin	ACACCCACCGCAGGCAGACGCAACGC CTCCGGAGACTAGCC	>100 pM	[151]
On	GO	AO	Hg ₂ ⁺	TGCTATCCCATCGGGTTGGGCGGGATGGGAT	0.17 nM	[152]
–	GO	ROX labeled aptamer	AFB1	GTTGGGCACGTGTTGTCTCTGTGTCTCGTG CCCTTCGCTAGGCCACA	10.0 ng/mL	[153]
Off-On	GO	FDNA aptamer	β-lactamase	CCAAACTCGGG	0.5 U/mL	[154]
	rGO	FAM labelled aptamer	Kanamycin	GCGCGCCACGGGCGCGC GCGCGGCGGCTACCCACCGCGCGC GGCGGTACCCACCG	1 pM	[155]
On	GO	QDs-aptamer	Ara h1	TGCACATTCCGCTTCTACCGGGGGGTCGAG CGAGTGAGCGAATCTGTGGTGGGCCGTAA GTCCGTGTGTGCGAA	56 ng/mL	[156]
On-Off	GO	Aptamer labeled Ag@SiO ₂ nanoparticles	Thrombin	TACGGTTGGTGTGGTTGG (Cy5-modified cDNA was also used as energy donor)	0.05 nM	[157]

donor and gold nanoclusters (AuNCs) with a 1.4 nm diameter as the acceptor molecules. According to the results, the distance between the acceptor and donor molecule connected with GA-specific aptamer was estimated to be 2 nm that reached up to 8 nm in the presence of the target molecule, GA. Consequently, the authors reported that the photoluminescence intensity increased with the increased concentration of GA, and a LoD of around 1 nM was achieved by such a design [39]. Jiang et al. [47], on the other hand, developed an RNA aptamer and AuNPs-based hybrid FRET assay for detection of Theophylline. Authors split the original theophylline aptamer from the loop regions into half in order to prevent nuclease degradation in serum. One part of the split RNA aptamer was attached to a DNA spacer strand composing of complementary Adenine and Thymine residues. The chimeric RNA/DNA structure was attached to the AuNPs

surface through PolyAdenine tail, and the other split half was modified with Cy3 fluorescent molecule, as represented in Fig. 7 [47]. Upon target binding, two structures came into close proximity, causing the fluorescent quenching of Cy3 and detection of Theophylline in nanomolar range with high selectivity. Recently, Li et al. utilized Palladium nanoparticles (PdNPs) despite the widespread use of AuNPs to detect alpha-fetoprotein using 5-carboxyfluorescein (FAM) labeled aptamers [161]. Although palladium nanoparticles does not show a specific plasmon absorption coinciding with the emission spectrum of FAM, the non-resonance wide-spectrum absorption of PdNPs were proven to be sufficient for biosensing.

LSPR modes depend on the size, shape and the dielectric properties of the surrounding medium [162]. Accordingly, AuNRs are also widely used for plasmonic absorption; since the position of their plasmonic resonance bands can easily be

Fig. 6 Aptamer-based nanoprobe in FRET. **a** Illustration of the steps taken for FRET-based GA detection; **(b)** Alteration in the distance between QDs and AuNPs in the absence and presence of GA. The figure was reused from Ref. [39]



controlled by tuning the aspect ratio of nanorods in the spectral range from 600 nm to 1300 nm [163]. AuNRs can absorb NIR photons more effectively than the other 2D acceptor materials [164]. NIR absorption property of AuNRs is important for applications like thrombin detection, where the background fluorescence might be strong and need to be avoided [82].

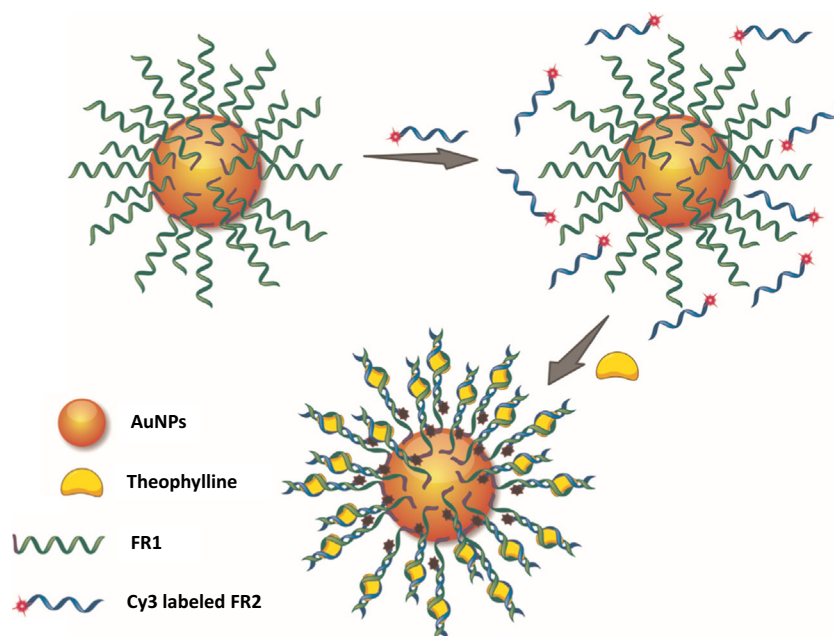
Recently, Chen et al. [96] reported a NaYF₄: Yb, Tm/NaGdF₄ core-shell UCNP donor/AuNRs acceptor based NIR-to-NIR energy transfer biosensor for detecting a cancer biomarker. In this study, the authors achieved a signal in NIR (804 nm) with a LoD of 0.17 ng/ml. Recently, Xing et al. [165] employed urchin-like AuNPs to achieve a NIR absorption in their sensor system for the detection of HER2 protein biomarker. Similarly, Zhang et al. [166] reported a study of using gold nanocrosses to obtain NIR absorption and used them for intercellular ATP detection. A couple of NSET systems based on the use of AuNPs and aptamers were summarized in Table 5.

Fluorescently-labeled aptamers can show some disadvantages. For example, covalent coupling process may be time-consuming, and it comes at a considerable cost. Equally important that there is a problem of interference between the fluorophore and target binding ability of the aptamer. In order

to tackle these issues, biosensors based on label-free aptamers have been developed. Among the assays related to “signal-on” label-free aptamers, one FRET experiment was designed for detection of *S. typhimurium* by using Rhodamine B (RB) and AuNPs [24]. Mixing of the target-specific aptamer and AuNPs with the RB were followed by the fluorescence-quenching of RB via FRET. Upon the addition of target, this bacterium binds with its aptamer and loses the capability of AuNPs stabilization; therefore, the salt causes the aggregation of AuNPs, resulting in the fluorescence recovery related to the quenched RB. The detection limit of 464 cfu/mL was achieved by this method.

Gold nanostructures offer great potential as NSET acceptors due to their shape-dependent optical properties and ease of chemical functionalization through thiol chemistry. Until now, most of the studies were limited to the spherical gold nanoparticles showing a plasmonic extinction wavelength band between 520 and 550 nm. However, other Au nanostructures such as nano urchins, nanorods, nanocrosses also dramatically increase the repertoire of plasmonic FRET acceptors. Considering the NSET mechanism and its larger energy transfer distances, the studies should evolve into the observation of the near-field response of these plasmonic structures to engineering better FRET acceptors.

Fig. 7 Detection of theophylline in serum using self-assembled RNA aptamer-based AuNPs nanoprobe RNA aptamer was split into two fragments as FR1 and FR2, which were used to bind with AuNPs and capture the target while maintaining the structure stable in serum. Adapted from [47]



Conclusion and Future Perspectives

FRET biosensors for clinical diagnosis, medical research, food monitoring, and environmental control can largely profit from sophisticated affinity probes with long shelf life and structural flexibility as well as nanoparticles with enhanced photophysical properties and biocompatible material compositions. The unique properties of nanomaterials and aptamers have made them versatile tools for FRET platforms with complementary benefits compared to organic dyes or antibodies. Although QDs and AuNPs are arguably the most applied nanoparticles for FRET biosensing, the repertoire of optoelectronic nanomaterials has broadened, and low-cost GQDs, anti-Stokes luminescent UCNPs, and graphene-based carbon

nanomaterials have become prominent FRET candidates. Aptamers have witnessed dramatic attraction after the recent expiration of SELEX patents, and it can be expected that their use in FRET-biosensing, together with other small artificial protein-based affinity probes [172, 173] will continue to complement antibodies in the future. Combining the structural simplicity and relatively small sizes of aptamers with the large surfaces and versatile optical properties of nanomaterials holds great potential to further improving FRET biosensors toward lower LoDs, higher sensitivities, and multiplexing. We anticipate that this triple nano biophotonic alliance (nanoparticles, aptamers, and FRET) will continue to provide exciting and useful high-fidelity biosensors for improved biological, chemical, medical and environmental analysis.

Table 5 Some of the AuNPs and aptamer-based energy transfer methods reported so far in the literature

Signal	Acceptor	Donor	Target	Aptamer	LoD	Ref.
On	AuNPs	UCNPs	<i>E. coli</i> ATCC 8739	GCAATGGTACGGTACTTCCCATGAGTGTGT GAAATGTTGGGACACTAGGTGGCATAGAGC CGCAAAGTGCACGCTACTTTGCTAA-NH ₂ SH-TTAGCAAAGTAGCGTGCACCTTTG	5–10 ⁶ cfu/mL	[42]
On	AuNPs	QDs	GA	TGCGGTTGTAGTACTCGTGCCG	1 nM	[39]
On	AuNPs	CDs	DNA	GGGGGGCCAAGGCCAGCCCTCACACA	15 fM	[167]
On	AuNPs	QDs	Chloramphenicol	ACTTCAGTGAGTTGTCCACGGTTCGGCGAGTC GGTGGTAG	3 pg/mL	[168]
On	Urchin-like AuNPs	QDs	HER2 protein	AAAAAAGCAGCGGTGTGGGGCAGCGGTGTGG GGGCAGCGGTGTGGGG	1 ng/mL	[165]
Off	AuNPs	AuNCs	<i>Staphylococcus aureus</i>	GCAATGGTACGGTACTTCCCTCGGCACGTTCTC AGTAGCGCTCGCTGGTCATCCACAGCTAC GTCAAAGTGCACGCTACTTTGCTAA	10 cfu/mL	[169]
On	AuNRs	QDs	Norovirus	GCGACGAATTAGCTTGTATGATGTCGTCGC	1.2 copy/mL	[170]
On	Au-Nano crosses	GQDs	ATP	ACTCCCCAGGT	0.27 mM	[166]
On	AuNPs	Ag NCs	Kanamycin	TGGGGTTGAGGCTAAGCCGA	1 nM	[171]

Compliance with ethical standards The author(s) declare that they have no competing interests.

Abbreviations AD, Adenosine; AFP, Alphafeto protein; AuNPs, Gold nanoparticles; AuNRs, Gold nanorods; AuNCs, Gold nanoclusters; BHQ1, Black Hole Quencher 1; BHQ2, Black Hole Quencher 2; cDNA, Complementary DNA; CDs, Carbon Dots; CEA, Carcinoembryonic antigen; CTC, Circulating tumor cells; EpCAM, Epithelial cell adhesion molecule; FAM, 5'-carboxyfluorescein; FRET, Förster resonance energy transfer; GA, Glycated albumin; GO, Graphene oxide; GQDs, Graphene quantum dots; LRET, Luminescence resonance energy transfer; LSPR, Localized surface plasmon resonance; MFNs, Magnetic fluorescent nanocomposite; MNPs, Metal nanoparticles; MOFs, Metal-organic frameworks; MoS₂, Molybdenum disulfide; NIR, Near-infrared Region; NSET, Nanosurface resonance energy transfer; OTA, Ochratoxin; QD, Quantum dot; RB, Rhodamine B; rGO, Reduced Graphene Oxide; rQD, Red-emitting QDs; gQDs, Green-emitting QDs; SELEX, Systematic evolution of ligands by exponential enrichment; ssDNA, Single-stranded DNA; TMD-NSs, Transition metal dichalcogenides nanosheets; UCNP, Upconverting nanoparticles; UV, Ultraviolet

References

- Qiu X, Hildebrandt N (2015) Rapid and Multiplexed MicroRNA Diagnostic Assay Using Quantum Dot-Based Förster Resonance Energy Transfer. *ACS Nano* 9:8449–8457. <https://doi.org/10.1021/acsnano.5b03364>
- He L, Lu D-Q, Liang H et al (2017) Fluorescence Resonance Energy Transfer-Based DNA Tetrahedron Nanotweezer for Highly Reliable Detection of Tumor-Related mRNA in Living Cells. *ACS Nano* 11:4060–4066. <https://doi.org/10.1021/acsnano.7b00725>
- Medintz I, Hildebrandt N (2014) FRET - Förster Resonance Energy Transfer. Wiley-VCH Verlag GmbH & Co, KGaA, Weinheim
- Clegg RM (1992) [18] Fluorescence resonance energy transfer and nucleic acids. In: *Methods in Enzymology*. Academic Press, pp 353–388
- Rowland CE, Brown CW, Medintz IL, Delehanty JB (2015) Intracellular FRET-based probes: a review. *Methods Appl Fluoresc* 3:042006. <https://doi.org/10.1088/2050-6120/3/4/042006>
- Hussain SA (2012) An Introduction to Fluorescence Resonance Energy Transfer (FRET). In: *arXiv.org*. <https://arxiv.org/abs/0908.1815>
- Gust A, Zander A, Gietl A et al (2014) A Starting Point for Fluorescence-Based Single-Molecule Measurements in Biomolecular Research. *Molecules* 19:15824–15865. <https://doi.org/10.3390/molecules191015824>
- Wen Y, Xing F, He S et al (2010) A graphene-based fluorescent nanoprobe for silver(i) ions detection by using graphene oxide and a silver-specific oligonucleotide. *Chem Commun* 46:2596. <https://doi.org/10.1039/b924832c>
- Kurt H, Alpaslan E, Yildiz B et al (2017) Conformation-mediated Förster resonance energy transfer (FRET) in blue-emitting polyvinylpyrrolidone (PVP)-passivated zinc oxide (ZnO) nanoparticles. *J Colloid Interface Sci* 488:348–355. <https://doi.org/10.1016/j.jcis.2016.11.017>
- Das P, Sedighi A, Krull UJ (2018) Cancer biomarker determination by resonance energy transfer using functional fluorescent nanoprobe. *Anal Chim Acta* 1041:1–24. <https://doi.org/10.1016/j.aca.2018.07.060>
- Amiri S, Ahmadi R, Salimi A et al (2018) Ultrasensitive and highly selective FRET aptasensor for Hg²⁺ measurement in fish samples using carbon dots/AuNPs as donor/acceptor platform. *New J Chem* 42:16027–16035. <https://doi.org/10.1039/C8NJ02781A>
- Kumar YVVA, R RM, A J et al (2018) Development of a FRET-based fluorescence aptasensor for the detection of aflatoxin B1 in contaminated food grain samples. *RSC Adv* 8:10465–10473. <https://doi.org/10.1039/C8RA00317C>
- Hildebrandt N, Spillmann CM, Algar WR et al (2017) Energy Transfer with Semiconductor Quantum Dot Bioconjugates: A Versatile Platform for Biosensing, Energy Harvesting, and Other Developing Applications. *Chem Rev* 117:536–711. <https://doi.org/10.1021/acs.chemrev.6b00030>
- Li Z, He M, Xu D, Liu Z (2014) Graphene materials-based energy acceptor systems and sensors. *J Photochem Photobiol C Photochem Rev* 18:1–17. <https://doi.org/10.1016/j.jphotochemrev.2013.10.002>
- Geißler D, Linden S, Liermann K et al (2014) Lanthanides and Quantum Dots as Förster Resonance Energy Transfer Agents for Diagnostics and Cellular Imaging. *Inorg Chem* 53:1824–1838. <https://doi.org/10.1021/ic4017883>
- Zu F, Yan F, Bai Z et al (2017) The quenching of the fluorescence of carbon dots: A review on mechanisms and applications. *Microchim. Acta* 184:1899–1914
- Khan IM, Zhao S, Niazi S et al (2018) Silver nanoclusters based FRET aptasensor for sensitive and selective fluorescent detection of T-2 toxin. *Sensors Actuators B Chem* 277:328–335. <https://doi.org/10.1016/j.snb.2018.09.021>
- Marx V (2017) Probes: FRET sensor design and optimization. *Nat Methods* 14:949–953. <https://doi.org/10.1038/nmeth.4434>
- Arruebo M, Valladares M, González-Fernández Á (2009) Antibody-Conjugated Nanoparticles for Biomedical Applications. *J Nanomater* 2009:1–24. <https://doi.org/10.1155/2009/439389>
- Yüce M, Ullah N, Budak H (2015) Trends in aptamer selection methods and applications. *Analyst* 140:5379–5399. <https://doi.org/10.1039/C5AN00954E>
- Yüce M, Kurt H (2017) How to make nanobiosensors: surface modification and characterisation of nanomaterials for biosensing applications. *RSC Adv* 7:49386–49403. <https://doi.org/10.1039/C7RA10479K>
- Mallikaratchy P (2017) Evolution of Complex Target SELEX to Identify Aptamers against Mammalian Cell-Surface Antigens. *Molecules* 22:215. <https://doi.org/10.3390/molecules22020215>
- Sun N, Ding Y, Tao Z et al (2018) Development of an upconversion fluorescence DNA probe for the detection of acetamiprid by magnetic nanoparticles separation. *Food Chem* 257:289–294. <https://doi.org/10.1016/j.foodchem.2018.02.148>
- Srinivasan S, Ranganathan V, DeRosa MC, Murari BM (2018) Label-free aptasensors based on fluorescent screening assays for the detection of Salmonella typhimurium. *Anal Biochem* 559:17–23. <https://doi.org/10.1016/j.ab.2018.08.002>
- Yüce M, Kurt H, Hussain B, Budak H (2018) Systematic Evolution of Ligands by Exponential Enrichment for Aptamer Selection. In: Sarmiento B, Das NJ (eds) *Biomedical Applications of Functionalized Nanomaterials*, 1st edn. Elsevier, pp 211–243
- Kurt H, Yüce M, Hussain B, Budak H (2016) Dual-excitation upconverting nanoparticle and quantum dot aptasensor for multiplexed food pathogen detection. *Biosens Bioelectron* 81:280–286. <https://doi.org/10.1016/j.bios.2016.03.005>

27. Yüce M, Kurt H, Hussain B et al (2018) Exploiting Stokes and anti-Stokes type emission profiles of aptamer-functionalized luminescent nanoprobes for multiplex sensing applications. *ChemistrySelect* 3:5814–5823. <https://doi.org/10.1002/slct.201801008>
28. Woo H-M, Lee J-M, Yim S, Jeong Y-J (2015) Isolation of Single-Stranded DNA Aptamers That Distinguish Influenza Virus Hemagglutinin Subtype H1 from H5. *PLoS One* 10:e0125060. <https://doi.org/10.1371/journal.pone.0125060>
29. Kim M, Um H-J, Bang S et al (2009) Arsenic Removal from Vietnamese Groundwater Using the Arsenic-Binding DNA Aptamer. *Environ Sci Technol* 43:9335–9340. <https://doi.org/10.1021/es902407g>
30. Savory N, Lednor D, Tsukakoshi K et al (2013) In silico maturation of binding-specificity of DNA aptamers against *Proteus mirabilis*. *Biotechnol Bioeng* 110:2573–2580. <https://doi.org/10.1002/bit.24922>
31. Li Z, Uzawa T, Tanaka T et al (2013) In vitro selection of peptide aptamers with affinity to single-wall carbon nanotubes using a ribosome display. *Biotechnol Lett* 35:39–45. <https://doi.org/10.1007/s10529-012-1049-6>
32. Lim YC, Kouzani AZ, Duan W (2009) Aptasensors Design Considerations. In: *Communications in Computer and Information Science*, pp 118–127
33. Chandra P, Noh H-B, Won M-S, Shim Y-B (2011) Detection of daunomycin using phosphatidylserine and aptamer co-immobilized on Au nanoparticles deposited conducting polymer. *Biosens Bioelectron* 26:4442–4449. <https://doi.org/10.1016/j.bios.2011.04.060>
34. Zhao W, Chiuman W, Brook MA, Li Y (2007) Simple and Rapid Colorimetric Biosensors Based on DNA Aptamer and Noncrosslinking Gold Nanoparticle Aggregation. *ChemBioChem* 8:727–731. <https://doi.org/10.1002/cbic.200700014>
35. Yang CJ, Jockusch S, Vicens M et al (2005) Light-switching excimer probes for rapid protein monitoring in complex biological fluids. *Proc Natl Acad Sci* 102:17278–17283. <https://doi.org/10.1073/pnas.0508821102>
36. Khati M (2010) The future of aptamers in medicine. *J Clin Pathol* 63:480–487. <https://doi.org/10.1136/jcp.2008.062786>
37. Dong H, Gao W, Yan F et al (2010) Fluorescence Resonance Energy Transfer between Quantum Dots and Graphene Oxide for Sensing Biomolecules. *Anal Chem* 82:5511–5517. <https://doi.org/10.1021/ac100852z>
38. Darbandi A, Datta D, Patel K et al (2017) Molecular beacon anchored onto a graphene oxide substrate. *Nanotechnology* 28:375501. <https://doi.org/10.1088/1361-6528/aa7e50>
39. Ghosh S, Datta D, Cheema M et al (2017) Aptasensor based optical detection of glycated albumin for diabetes mellitus diagnosis. *Nanotechnology* 28:435505. <https://doi.org/10.1088/1361-6528/aa893a>
40. Li S, Xu L, Ma W et al (2016) Dual-Mode Ultrasensitive Quantification of MicroRNA in Living Cells by Chiroplasmic Nanopyramids Self-Assembled from Gold and Upconversion Nanoparticles. *J Am Chem Soc* 138:306–312. <https://doi.org/10.1021/jacs.5b10309>
41. Li M, Zhou X, Guo S, Wu N (2013) Detection of lead (II) with a “turn-on” fluorescent biosensor based on energy transfer from CdSe/ZnS quantum dots to graphene oxide. *Biosens Bioelectron* 43:69–74. <https://doi.org/10.1016/j.bios.2012.11.039>
42. Jin B, Wang S, Lin M et al (2017) Upconversion nanoparticles based FRET aptasensor for rapid and ultrasensitive bacteria detection. *Biosens Bioelectron* 90:525–533. <https://doi.org/10.1016/j.bios.2016.10.029>
43. Yang W, Zhang G, Weng W et al (2014) Signal on fluorescence biosensor for MMP-2 based on FRET between semiconducting polymer dots and a metal organic framework. *RSC Adv* 4:58852–58857. <https://doi.org/10.1039/C4RA12478B>
44. Wang Y, Bao L, Liu Z, Pang D-W (2011) Aptamer Biosensor Based on Fluorescence Resonance Energy Transfer from Upconverting Phosphors to Carbon Nanoparticles for Thrombin Detection in Human Plasma. *Anal Chem* 83:8130–8137. <https://doi.org/10.1021/ac201631b>
45. Li X-HH, Sun W-MM, Wu J et al (2018) An ultrasensitive fluorescence aptasensor for carcino-embryonic antigen detection based on fluorescence resonance energy transfer from upconversion phosphors to Au nanoparticles. *Anal Methods* 10:1552–1559. <https://doi.org/10.1039/C7AY02803B>
46. Ueno Y, Furukawa K, Tin A, Hibino H (2015) On-chip FRET Graphene Oxide Aptasensor: Quantitative Evaluation of Enhanced Sensitivity by Aptamer with a Double-stranded DNA Spacer. *Anal Sci* 31:875–879. <https://doi.org/10.2116/analsci.31.875>
47. Jiang H, Ling K, Tao X, Zhang Q (2015) Theophylline detection in serum using a self-assembling RNA aptamer-based gold nanoparticle sensor. *Biosens Bioelectron* 70:299–303. <https://doi.org/10.1016/j.bios.2015.03.054>
48. Kim B, Malioutov DM, Varshney KR, Weller A (2017) Proceedings of the 2017 ICML Workshop on Human Interpretability in Machine Learning (WHI 2017). *New J Chem* 37:3998. <https://doi.org/10.1039/c3nj00594a>
49. Ahar MJ (2017) A Review on Aptamer-Conjugated Quantum Dot Nanosystems for Cancer Imaging and Theranostic. *J Nanomedicine Res* 5. <https://doi.org/10.15406/jnmr.2017.05.00117>
50. Michalet X (2005) Quantum Dots for Live Cells, in Vivo Imaging, and Diagnostics. *Science* (80-) 307:538–544. <https://doi.org/10.1126/science.1104274>
51. Zeng Z, Garoufalis CS, Terzis AF, Baskoutas S (2013) Linear and nonlinear optical properties of ZnO/ZnS and ZnS/ZnO core shell quantum dots: Effects of shell thickness, impurity, and dielectric environment. *J Appl Phys* 114:023510. <https://doi.org/10.1063/1.4813094>
52. Vasudevan D, Gaddam RR, Trinchi A, Cole I (2015) Core-shell quantum dots: Properties and applications. *J Alloys Compd* 636:395–404. <https://doi.org/10.1016/j.jallcom.2015.02.102>
53. Fang B-Y, Wang C-Y, Li C et al (2017) Amplified using DNase I and aptamer/graphene oxide for sensing prostate specific antigen in human serum. *Sensors Actuators B Chem* 244:928–933. <https://doi.org/10.1016/j.snb.2017.01.045>
54. Medintz IL, Uyeda HT, Goldman ER, Mattoussi H (2005) Quantum dot bioconjugates for imaging, labelling and sensing. *Nat Mater* 4:435–446. <https://doi.org/10.1038/nmat1390>
55. Zhang C, Ding C, Zhou G et al (2017) One-step synthesis of DNA functionalized cadmium-free quantum dots and its application in FRET-based protein sensing. *Anal Chim Acta* 957:63–69. <https://doi.org/10.1016/j.aca.2016.12.024>
56. Arvand M, Mirroshandel AA (2017) Highly-sensitive aptasensor based on fluorescence resonance energy transfer between l -cysteine capped ZnS quantum dots and graphene oxide sheets for the determination of edifenphos fungicide. *Biosens Bioelectron* 96:324–331. <https://doi.org/10.1016/j.bios.2017.05.028>
57. Duan N, Wu S, Dai S et al (2015) Simultaneous detection of pathogenic bacteria using an aptamer based biosensor and dual fluorescence resonance energy transfer from quantum dots to carbon nanoparticles. *Microchim Acta* 182:917–923. <https://doi.org/10.1007/s00604-014-1406-3>

58. Das P, Krull UJ (2017) Detection of a cancer biomarker protein on modified cellulose paper by fluorescence using aptamer-linked quantum dots. *Analyst* 142:3132–3135. <https://doi.org/10.1039/c7an00624a>
59. Sabet FS, Hosseini M, Khabbaz H et al (2017) FRET-based aptamer biosensor for selective and sensitive detection of aflatoxin B1 in peanut and rice. *Food Chem* 220:527–532. <https://doi.org/10.1016/j.foodchem.2016.10.004>
60. Hildebrandt N, Charbonnière LJ, Beck M et al (2005) Quantum Dots as Efficient Energy Acceptors in a Time-Resolved Fluoroimmunoassay. *Angew Chemie Int Ed* 44:7612–7615. <https://doi.org/10.1002/anie.200501552>
61. So M-K, Xu C, Loening AM et al (2006) Self-illuminating quantum dot conjugates for in vivo imaging. *Nat Biotechnol* 24:339–343. <https://doi.org/10.1038/nbt1188>
62. Doughan S, Uddayasankar U, Krull UJ (2015) A paper-based resonance energy transfer nucleic acid hybridization assay using upconversion nanoparticles as donors and quantum dots as acceptors. *Anal Chim Acta* 878:1–8. <https://doi.org/10.1016/j.aca.2015.04.036>
63. Qiu X, Guo J, Jin Z et al (2017) Multiplexed Nucleic Acid Hybridization Assays Using Single-FRET-Pair Distance-Tuning. *Small* 13:1700332. <https://doi.org/10.1002/sml.201700332>
64. Qiu X, Guo J, Xu J, Hildebrandt N (2018) Three-Dimensional FRET Multiplexing for DNA Quantification with Attomolar Detection Limits. *J Phys Chem Lett* 9:4379–4384. <https://doi.org/10.1021/acs.jpcclett.8b01944>
65. Qiu X, Xu J, Guo J et al (2018) Advanced microRNA-based cancer diagnostics using amplified time-gated FRET. *Chem Sci* 9:8046–8055. <https://doi.org/10.1039/C8SC03121E>
66. Guo J, Qiu X, Mingoies C et al (2019) Conformational Details of Quantum Dot-DNA Resolved by Förster Resonance Energy Transfer Lifetime Nanoruler. *ACS Nano* 13:505–514. <https://doi.org/10.1021/acsnano.8b07137>
67. Doughan S, Han Y, Uddayasankar U, Krull UJ (2014) Solid-phase covalent immobilization of upconverting nanoparticles for biosensing by luminescence resonance energy transfer. *ACS Appl Mater Interfaces* 6:14061–14068. <https://doi.org/10.1021/am503391m>
68. Li Y, Xu J, Wang L et al (2016) Aptamer-based fluorescent detection of bisphenol A using nonconjugated gold nanoparticles and CdTe quantum dots. *Sensors Actuators, B Chem* 222:815–822. <https://doi.org/10.1016/j.snb.2015.08.130>
69. Tianyu H, Xu Y, Weidan N, Xingguang S (2016) Aptamer-based aggregation assay for mercury(II) using gold nanoparticles and fluorescent CdTe quantum dots. *Microchim Acta* 183:2131–2137. <https://doi.org/10.1007/s00604-016-1831-6>
70. Lu X, Wang C, Qian J et al (2019) Target-driven switch-on fluorescence aptasensor for trace aflatoxin B1 determination based on highly fluorescent ternary CdZnTe quantum dots. *Anal Chim Acta* 1047:163–171. <https://doi.org/10.1016/j.aca.2018.10.002>
71. Kavosi B, Navaee A, Salimi A (2018) Amplified fluorescence resonance energy transfer sensing of prostate specific antigen based on aggregation of CdTe QDs/antibody and aptamer decorated of AuNPs-PAMAM dendrimer. *J Lumin* 204:368–374. <https://doi.org/10.1016/j.jlumin.2018.08.012>
72. Lu Z, Chen X, Hu W (2017) A fluorescence aptasensor based on semiconductor quantum dots and MoS2 nanosheets for ochratoxin A detection. *Sensors Actuators B Chem* 246:61–67. <https://doi.org/10.1016/j.snb.2017.02.062>
73. Qiu Z, Shu J, He Y et al (2017) CdTe/CdSe quantum dot-based fluorescent aptasensor with hemin/G-quadruplex DNzyme for sensitive detection of lysozyme using rolling circle amplification and strand hybridization. *Biosens Bioelectron* 87:18–24. <https://doi.org/10.1016/j.bios.2016.08.003>
74. Lu Z, Chen X, Wang Y et al (2015) Aptamer based fluorescence recovery assay for aflatoxin B1 using a quencher system composed of quantum dots and graphene oxide. *Microchim Acta* 182:571–578. <https://doi.org/10.1007/s00604-014-1360-0>
75. Xiang L, Tang J (2017) QD-aptamer as a donor for a FRET-based chemosensor and evaluation of affinity between acetamiprid and its aptamer. *RSC Adv* 7:8332–8337. <https://doi.org/10.1039/c6ra26118c>
76. Li Y, Su R, Xu J et al (2018) Aptamers-Based Sensing Strategy for 17 β -Estradiol Through Fluorescence Resonance Energy Transfer Between Oppositely Charged CdTe Quantum Dots and Gold Nanoparticles. *J Nanosci Nanotechnol* 18:1517–1527. <https://doi.org/10.1166/jnn.2018.14235>
77. Hu W, Chen Q, Li H et al (2016) Fabricating a novel label-free aptasensor for acetamiprid by fluorescence resonance energy transfer between NH₂-NaYF₄:Yb, Ho@SiO₂ and Au nanoparticles. *Biosens Bioelectron* 80:398–404. <https://doi.org/10.1016/j.bios.2016.02.001>
78. Tu L, Liu X, Wu F, Zhang H (2015) Excitation energy migration dynamics in upconversion nanomaterials. *Chem Soc Rev* 44:1331–1345. <https://doi.org/10.1039/c4cs00168k>
79. Zhou B, Shi B, Jin D, Liu X (2015) Controlling upconversion nanocrystals for emerging applications. *Nat. Nanotechnol.* 10:924–936
80. Chen H, Guan Y, Wang S et al (2014) Turn-On Detection of a Cancer Marker Based on Near-Infrared Luminescence Energy Transfer from NaYF₄:Yb,Tm/NaGdF₄ Core-Shell Upconverting Nanoparticles to Gold Nanorods. *Langmuir* 30:13085–13091. <https://doi.org/10.1021/la502753e>
81. Li C, Zuo J, Li Q et al (2017) One-step in situ solid-substrate-based whole blood immunoassay based on FRET between upconversion and gold nanoparticles. *Biosens Bioelectron* 92:335–341. <https://doi.org/10.1016/j.bios.2016.11.003>
82. Chen H, Yuan F, Wang S et al (2013) Aptamer-based sensing for thrombin in red region via fluorescence resonant energy transfer between NaYF₄:Yb,Er upconversion nanoparticles and gold nanorods. *Biosens Bioelectron* 48:19–25. <https://doi.org/10.1016/j.bios.2013.03.083>
83. Hwang S-H, Im S-G, Sung H et al (2014) Upconversion nanoparticle-based Förster resonance energy transfer for detecting the IS6110 sequence of *Mycobacterium tuberculosis* complex in sputum. *Biosens Bioelectron* 53:112–116. <https://doi.org/10.1016/j.bios.2013.09.011>
84. Vilela P, El-Sagheer A, Millar TM et al (2017) Graphene Oxide-Upconversion Nanoparticle Based Optical Sensors for Targeted Detection of mRNA Biomarkers Present in Alzheimer's Disease and Prostate Cancer. *ACS Sensors* 2:52–56. <https://doi.org/10.1021/acssensors.6b00651>
85. Ye WW, Tsang M-K, Liu X et al (2014) Upconversion Luminescence Resonance Energy Transfer (LRET)-Based Biosensor for Rapid and Ultrasensitive Detection of Avian Influenza Virus H7 Subtype. *Small* 10:2390–2397. <https://doi.org/10.1002/sml.201303766>
86. Long Q, Li H, Zhang Y, Yao S (2015) Upconversion nanoparticle-based fluorescence resonance energy transfer assay for organophosphorus pesticides. *Biosens Bioelectron* 68:168–174. <https://doi.org/10.1016/j.bios.2014.12.046>
87. Li H, Sun D, Liu Y, Liu Z (2014) An ultrasensitive homogeneous aptasensor for kanamycin based on upconversion fluorescence resonance energy transfer. *Biosens Bioelectron* 55:149–156. <https://doi.org/10.1016/j.bios.2013.11.079>
88. Cheng K, Zhang J, Zhang L et al (2017) Aptamer biosensor for Salmonella typhimurium detection based on luminescence energy transfer from Mn²⁺-doped NaYF₄:Yb, Tm upconverting nanoparticles to gold nanorods. *Spectrochim Acta Part A Mol Biomol Spectrosc* 171:168–173. <https://doi.org/10.1016/j.saa.2016.08.012>

89. Hao T, Wu X, Xu L et al (2017) Ultrasensitive Detection of Prostate-Specific Antigen and Thrombin Based on Gold-Upconversion Nanoparticle Assembled Pyramids. *Small* 13: 1603944. <https://doi.org/10.1002/sml.201603944>
90. Qu A, Wu X, Xu L et al (2017) SERS- and luminescence-active Au–Au–UCNP trimers for attomolar detection of two cancer biomarkers. *Nanoscale* 9:3865–3872. <https://doi.org/10.1039/C6NR09114H>
91. Zhang H, Fang C, Wu S et al (2015) Upconversion luminescence resonance energy transfer-based aptasensor for the sensitive detection of oxytetracycline. *Anal Biochem* 489:44–49. <https://doi.org/10.1016/j.ab.2015.08.011>
92. Liu Y, Ouyang Q, Li H et al (2018) Turn-On Fluorescence Sensor for Hg²⁺ in Food Based on FRET between Aptamers-Functionalized Upconversion Nanoparticles and Gold Nanoparticles. *J Agric Food Chem* 66:6188–6195. <https://doi.org/10.1021/acs.jafc.8b00546>
93. Wang Y, Wei Z, Luo X et al (2019) An ultrasensitive homogeneous aptasensor for carcinoembryonic antigen based on upconversion fluorescence resonance energy transfer. *Talanta* 195:33–39. <https://doi.org/10.1016/j.talanta.2018.11.011>
94. Wu S, Duan N, Zhang H, Wang Z (2015) Simultaneous detection of microcystin-LR and okadaic acid using a dual fluorescence resonance energy transfer aptasensor. *Anal Bioanal Chem* 407:1303–1312. <https://doi.org/10.1007/s00216-014-8378-3>
95. Wu Z, Xu E, Jin Z, Irudayaraj J (2018) An ultrasensitive aptasensor based on fluorescent resonant energy transfer and exonuclease-assisted target recycling for patulin detection. *Food Chem* 249: 136–142. <https://doi.org/10.1016/j.foodchem.2018.01.025>
96. Li H, Shi L, en SD et al (2016) Fluorescence resonance energy transfer biosensor between upconverting nanoparticles and palladium nanoparticles for ultrasensitive CEA detection. *Biosens Bioelectron* 86:791–798. <https://doi.org/10.1016/j.bios.2016.07.070>
97. Dai S, Wu S, Duan N, Wang Z (2016) A luminescence resonance energy transfer based aptasensor for the mycotoxin Ochratoxin A using upconversion nanoparticles and gold nanorods. *Microchim Acta* 183:1909–1916. <https://doi.org/10.1007/s00604-016-1820-9>
98. Smith NM, Amrane S, Rosu F et al (2012) Mercury–thymine interaction with a chair type G-quadruplex architecture. *Chem Commun* 48:11464. <https://doi.org/10.1039/c2cc36481f>
99. Büning-Pfaue H (2003) Analysis of water in food by near infrared spectroscopy. *Food Chem* 82:107–115. [https://doi.org/10.1016/S0308-8146\(02\)00583-6](https://doi.org/10.1016/S0308-8146(02)00583-6)
100. Kong L, Li Y, Ma C et al (2018) Sensitive immunoassay of von Willebrand factor based on fluorescence resonance energy transfer between graphene quantum dots and Ag@Au nanoparticles. *Colloids Surfaces B Biointerfaces* 165:286–292. <https://doi.org/10.1016/j.colsurfb.2018.02.049>
101. Gao X, Zhang B, Zhang Q et al (2018) The influence of combination mode on the structure and properties of graphene quantum dot-porphyrin composites. *Colloids Surfaces B Biointerfaces* 172: 207–212. <https://doi.org/10.1016/j.colsurfb.2018.08.010>
102. He Y, Wen X, Zhang B, Fan Z (2018) Novel aptasensor for the ultrasensitive detection of kanamycin based on graphene oxide quantum-dot-linked single-stranded DNA-binding protein. *Sensors Actuators, B Chem* 265:20–26. <https://doi.org/10.1016/j.snb.2018.03.029>
103. Shen J, Zhu Y, Yang X, Li C (2012) Graphene quantum dots: emergent nanolights for bioimaging, sensors, catalysis and photovoltaic devices. *Chem Commun* 48:3686. <https://doi.org/10.1039/c2cc00110a>
104. Shi J, Chan C, Pang Y et al (2015) A fluorescence resonance energy transfer (FRET) biosensor based on graphene quantum dots (GQDs) and gold nanoparticles (AuNPs) for the detection of mecA gene sequence of *Staphylococcus aureus*. *Biosens Bioelectron* 67:595–600. <https://doi.org/10.1016/j.bios.2014.09.059>
105. Shen J, Zhu Y, Yang X et al (2012) One-pot hydrothermal synthesis of graphenequantum dots surface-passivated by polyethylene glycol and their photoelectric conversion under near-infrared light. *New J Chem* 36:97–101. <https://doi.org/10.1039/C1NJ20658C>
106. Shi J, Lyu J, Tian F, Yang M (2017) A fluorescence turn-on biosensor based on graphene quantum dots (GQDs) and molybdenum disulfide (MoS₂) nanosheets for epithelial cell adhesion molecule (EpCAM) detection. *Biosens Bioelectron* 93:182–188. <https://doi.org/10.1016/j.bios.2016.09.012>
107. Pfeiffer F, Mayer G (2016) Selection and Biosensor Application of Aptamers for Small Molecules. *Front Chem* 4(25). <https://doi.org/10.3389/fchem.2016.00025>
108. Pfohl-Leskowicz A, Manderville RA (2007) Ochratoxin A: An overview on toxicity and carcinogenicity in animals and humans. *Mol Nutr Food Res* 51:61–99. <https://doi.org/10.1002/mnfr.200600137>
109. Cao L-H, Li H-Y, Xu H et al (2017) Diverse dissolution–recrystallization structural transformations and sequential Förster resonance energy transfer behavior of a luminescent porous Cd-MOF. *Dalt Trans* 46:11656–11663. <https://doi.org/10.1039/C7DT02697H>
110. Tian J, Wei W, Wang J et al (2018) Fluorescence resonance energy transfer aptasensor between nanoceria and graphene quantum dots for the determination of ochratoxin A. *Anal Chim Acta* 1000:265–272. <https://doi.org/10.1016/j.aca.2017.08.018>
111. Cheng X, Cen Y, Xu G et al (2018) Aptamer based fluorometric determination of ATP by exploiting the FRET between carbon dots and graphene oxide. *Microchim Acta* 185(144). <https://doi.org/10.1007/s00604-018-2683-z>
112. Wu X, Song Y, Yan X et al (2017) Carbon quantum dots as fluorescence resonance energy transfer sensors for organophosphate pesticides determination. *Biosens Bioelectron* 94:292–297. <https://doi.org/10.1016/j.bios.2017.03.010>
113. Mohammadi S, Salimi A, Hamd-Ghadareh S et al (2018) A FRET immunosensor for sensitive detection of CA 15–3 tumor marker in human serum sample and breast cancer cells using antibody functionalized luminescent carbon-dots and AuNPs-dendrimer aptamer as donor-acceptor pair. *Anal Biochem* 557:18–26. <https://doi.org/10.1016/j.ab.2018.06.008>
114. Zhu S, Song Y, Zhao X et al (2015) The photoluminescence mechanism in carbon dots (graphene quantum dots, carbon nanodots, and polymer dots): current state and future perspective. *Nano Res* 8:355–381
115. Wang X, Xu G, Wei F et al (2017) Highly sensitive and selective aptasensor for detection of adenosine based on fluorescence resonance energy transfer from carbon dots to nano-graphite. *J Colloid Interface Sci* 508:455–461. <https://doi.org/10.1016/j.jcis.2017.07.028>
116. Zhao Q, Zhou C, Yang Q et al (2019) A FRET-based fluorescent probe for hydrogen peroxide based on the use of carbon quantum dots conjugated to gold nanoclusters. *Microchim Acta* 186(294). <https://doi.org/10.1007/s00604-019-3398-5>
117. Qian ZS, Shan XY, Chai LJ et al (2015) A fluorescent nanosensor based on graphene quantum dots–aptamer probe and graphene oxide platform for detection of lead (II) ion. *Biosens Bioelectron* 68:225–231. <https://doi.org/10.1016/j.bios.2014.12.057>
118. Saberi Z, Rezaei B, Faroukhpour H, Ensafi AA (2018) A fluorometric aptasensor for methamphetamine based on fluorescence resonance energy transfer using cobalt oxyhydroxide nanosheets and carbon dots. *Microchim Acta* 185:303. <https://doi.org/10.1007/s00604-018-2842-2>
119. Shen X, Xu L, Zhu W et al (2017) A turn-on fluorescence aptasensor based on carbon dots for sensitive detection of adenosine. *New J Chem* 41:9230–9235. <https://doi.org/10.1039/C7NJ02384G>

120. Xu M, Gao Z, Zhou Q et al (2016) Terbium ion-coordinated carbon dots for fluorescent aptasensing of adenosine 5'-triphosphate with unmodified gold nanoparticles. *Biosens Bioelectron* 86:978–984. <https://doi.org/10.1016/j.bios.2016.07.105>
121. Zhu L, Xu G, Song Q et al (2016) Highly sensitive determination of dopamine by a turn-on fluorescent biosensor based on aptamer labeled carbon dots and nano-graphite. *Sensors Actuators B Chem* 231:506–512. <https://doi.org/10.1016/j.snb.2016.03.084>
122. Wang B, Chen Y, Wu Y et al (2016) Aptamer induced assembly of fluorescent nitrogen-doped carbon dots on gold nanoparticles for sensitive detection of AFB 1. *Biosens Bioelectron* 78:23–30. <https://doi.org/10.1016/j.bios.2015.11.015>
123. Wang Y, Ma T, Ma S et al (2017) Fluorometric determination of the antibiotic kanamycin by aptamer-induced FRET quenching and recovery between MoS₂nanosheets and carbon dots. *Microchim Acta* 184:203–210. <https://doi.org/10.1007/s00604-016-2011-4>
124. Zhu X, Zheng H, Wei X et al (2013) Metal–organic framework (MOF): a novel sensing platform for biomolecules. *Chem Commun* 49:1276. <https://doi.org/10.1039/c2cc36661d>
125. McKinlay AC, Morris RE, Horcajada P et al (2010) BioMOFs: Metal-Organic Frameworks for Biological and Medical Applications. *Angew Chemie Int Ed* 49:6260–6266. <https://doi.org/10.1002/anie.201000048>
126. Ma D, Wang W, Li Y et al (2010) In situ 2,5-pyrazinedicarboxylate and oxalate ligands synthesis leading to a microporous europium–organic framework capable of selective sensing of small molecules. *CrystEngComm* 12:4372. <https://doi.org/10.1039/c0ce00135j>
127. Qu F, Sun C, Lv X, You J (2018) A terbium-based metal-organic framework@gold nanoparticle system as a fluorometric probe for aptamer based determination of adenosine triphosphate. *Mikrochim Acta* 185:359. <https://doi.org/10.1007/s00604-018-2888-1>
128. Lee J, Kim J, Kim S, Min DH (2016) Biosensors based on graphene oxide and its biomedical application. *Adv. Drug Deliv. Rev.* 105:275–287
129. Zou W, Gong F, Gu T et al (2018) An efficient strategy for sensing pyrophosphate based on nitrogen-rich quantum dots combined with graphene oxide. *Microchem J* 141:466–472. <https://doi.org/10.1016/j.microc.2018.06.004>
130. Dhiman A, Kalra P, Bansal V et al (2017) Aptamer-based point-of-care diagnostic platforms. *Sensors Actuators, B Chem.* 246:535–553
131. Lee J, Samson AAS, Yim Y et al (2019) A FRET assay for the quantitation of inhibitors of exonuclease EcoRV by using parchment paper inkjet-printed with graphene oxide and FAM-labelled DNA. *Microchim Acta* 186(211). <https://doi.org/10.1007/s00604-019-3317-9>
132. Alonso-Cristobal P, Vilela P, El-Sagheer A et al (2015) Highly Sensitive DNA Sensor Based on Upconversion Nanoparticles and Graphene Oxide. *ACS Appl Mater Interfaces* 7:12422–12429. <https://doi.org/10.1021/am507591u>
133. Furukawa K, Ueno Y, Takamura M, Hibino H (2016) Graphene FRET Aptasensor. *ACS Sensors* 1:710–716. <https://doi.org/10.1021/acssensors.6b00191>
134. Tian F, Lyu J, Shi J, Yang M (2017) Graphene and graphene-like two-denominational materials based fluorescence resonance energy transfer (FRET) assays for biological applications. *Biosens Bioelectron* 89:123–135. <https://doi.org/10.1016/j.bios.2016.06.046>
135. García-Cañas V, Simó C, Herrero M et al (2012) Present and Future Challenges in Food Analysis: Foodomics. *Anal Chem* 84:10150–10159. <https://doi.org/10.1021/ac301680q>
136. Arnold SM, Clark KE, Staples CA et al (2013) Relevance of drinking water as a source of human exposure to bisphenol A. *J Expo Sci Environ Epidemiol* 23:137–144. <https://doi.org/10.1038/jes.2012.66>
137. Zhu Y, Cai Y, Xu L et al (2015) Building An Aptamer/Graphene Oxide FRET Biosensor for One-Step Detection of Bisphenol A. *ACS Appl Mater Interfaces* 7:7492–7496. <https://doi.org/10.1021/acscami.5b00199>
138. Zhang H, Zhang H, Aldalbah A et al (2017) Fluorescent biosensors enabled by graphene and graphene oxide. *Biosens Bioelectron* 89:96–106. <https://doi.org/10.1016/j.bios.2016.07.030>
139. Zhou ZM, Zhou J, Chen J et al (2014) Carcino-embryonic antigen detection based on fluorescence resonance energy transfer between quantum dots and graphene oxide. *Biosens Bioelectron* 59:397–403. <https://doi.org/10.1016/j.bios.2014.04.002>
140. Kenry GA, Zhang X et al (2016) Highly Sensitive and Selective Aptamer-Based Fluorescence Detection of a Malarial Biomarker Using Single-Layer MoS₂Nanosheets. *ACS Sensors* 1:1315–1321. <https://doi.org/10.1021/acssensors.6b00449>
141. Singh P, Gupta R, Sinha M et al (2016) MoS₂based digital response platform for aptamer based fluorescent detection of pathogens. *Microchim Acta* 183:1501–1506. <https://doi.org/10.1007/s00604-016-1762-2>
142. Yuan Y, Li R, Liu Z (2014) Establishing water-soluble layered WS₂ nanosheet as a platform for biosensing. *Anal Chem* 86:3610–3615. <https://doi.org/10.1021/ac5002096>
143. Zhang Y, Zheng B, Zhu C et al (2015) Single-Layer Transition Metal Dichalcogenide Nanosheet-Based Nanosensors for Rapid, Sensitive, and Multiplexed Detection of DNA. *Adv Mater* 27:935–939. <https://doi.org/10.1002/adma.201404568>
144. Ge J, Ou E-C, Yu R-Q, Chu X (2014) A novel aptameric nanobiosensor based on the self-assembled DNA–MoS₂ nanosheet architecture for biomolecule detection. *J Mater Chem B* 2:625–628. <https://doi.org/10.1039/C3TB21570A>
145. Cui F, Ji J, Sun J et al (2019) A novel magnetic fluorescent biosensor based on graphene quantum dots for rapid, efficient, and sensitive separation and detection of circulating tumor cells. *Anal Bioanal Chem* 411:985–995. <https://doi.org/10.1007/s00216-018-1501-0>
146. Gao L, Li Q, Deng Z et al (2017) Highly sensitive protein detection via covalently linked aptamer to MoS₂ and exonuclease-assisted amplification strategy. *Int J Nanomedicine* 12:7847–7853. <https://doi.org/10.2147/IJN.S145585>
147. Jia L, Ding L, Tian J et al (2015) Aptamer loaded MoS₂ nanoplates as nanoprobe for detection of intracellular ATP and controllable photodynamic therapy. *Nanoscale* 7:15953–15961. <https://doi.org/10.1039/C5NR02224J>
148. Ravikumar A, Panneerselvam P, Radhakrishnan K et al (2018) MoS₂ nanosheets as an effective fluorescent quencher for successive detection of arsenic ions in aqueous system. *Appl Surf Sci* 449:31–38. <https://doi.org/10.1016/j.apsusc.2017.12.098>
149. Xu S, Feng X, Gao T et al (2017) Aptamer induced multicoloured Au NCs–MoS₂ “switch on” fluorescence resonance energy transfer biosensor for dual color simultaneous detection of multiple tumor markers by single wavelength excitation. *Anal Chim Acta* 983:173–180. <https://doi.org/10.1016/j.aca.2017.06.023>
150. Chen J, Li Y, Huang Y et al (2019) Fluorometric dopamine assay based on an energy transfer system composed of aptamer-functionalized MoS₂ quantum dots and MoS₂ nanosheets. *Microchim Acta* 186(58). <https://doi.org/10.1007/s00604-018-3143-5>
151. Esteban-Fernández de Ávila B, Lopez-Ramirez MA, Báez DF et al (2016) Aptamer-Modified Graphene-Based Catalytic Micromotors: Off–On Fluorescent Detection of Ricin. *ACS Sensors* 1:217–221. <https://doi.org/10.1021/acssensors.5b00300>

152. Guo H, Li J, Li Y et al (2018) A turn-on fluorescent sensor for Hg²⁺ detection based on graphene oxide and DNA aptamers. *New J Chem* 42:11147–11152. <https://doi.org/10.1039/C8NJ01709C>
153. Zhang J, Li Z, Zhao S, Lu Y (2016) Size-dependent modulation of graphene oxide–aptamer interactions for an amplified fluorescence-based detection of aflatoxin B 1 with a tunable dynamic range. *Analyst* 141:4029–4034. <https://doi.org/10.1039/C6AN00368K>
154. Qin J, Cui X, Wu P et al (2017) Fluorescent sensor assay for β -lactamase in milk based on a combination of aptamer and graphene oxide. *Food Control* 73:726–733. <https://doi.org/10.1016/j.foodcont.2016.09.023>
155. Ha N, Jung I-P, La I et al (2017) Ultra-sensitive detection of kanamycin for food safety using a reduced graphene oxide-based fluorescent aptasensor. *Sci Rep* 7(40305). <https://doi.org/10.1038/srep40305>
156. Weng X, Neethirajan S (2016) A microfluidic biosensor using graphene oxide and aptamer-functionalized quantum dots for peanut allergen detection. *Biosens Bioelectron* 85:649–656. <https://doi.org/10.1016/j.bios.2016.05.072>
157. Sui N, Wang L, Xie F et al (2016) Ultrasensitive aptamer-based thrombin assay based on metal enhanced fluorescence resonance energy transfer. *Microchim Acta* 183:1563–1570. <https://doi.org/10.1007/s00604-016-1774-y>
158. Persson BNJ, Lang ND (1982) Electron-hole-pair quenching of excited states near a metal. *Phys Rev B* 26:5409–5415. <https://doi.org/10.1103/PhysRevB.26.5409>
159. Chen C, Midelet C, Bhuckory S et al (2018) Nanosurface Energy Transfer from Long-Lifetime Terbium Donors to Gold Nanoparticles. *J Phys Chem C* 122:17566–17574. <https://doi.org/10.1021/acs.jpcc.8b06539>
160. Jennings TL, Singh MP, Strouse GF (2006) Fluorescent Lifetime Quenching near $d = 1.5$ nm Gold Nanoparticles: Probing NSET Validity. *J Am Chem Soc* 128:5462–5467. <https://doi.org/10.1021/ja0583665>
161. Li G, Zeng J, Liu H et al (2019) A fluorometric aptamer nanoprobe for alpha-fetoprotein by exploiting the FRET between 5-carboxyfluorescein and palladium nanoparticles. *Microchim Acta* 186(314). <https://doi.org/10.1007/s00604-019-3403-z>
162. Holzinger M, Le Goff A, Cosnier S (2014) Nanomaterials for biosensing applications: a review. *Front Chem* 2:1–10. <https://doi.org/10.3389/fchem.2014.00063>
163. Abouna GM (2004) The use of marginal-suboptimal donor organs: a practical solution for organ shortage. *Ann Transplant* 9: 62–66. <https://doi.org/10.1021/cm020732l>
164. Yuan F, Chen H, Xu J et al (2014) Aptamer-Based Luminescence Energy Transfer from Near-Infrared-to-Near-Infrared Upconverting Nanoparticles to Gold Nanorods and Its Application for the Detection of Thrombin. *Chem - A Eur J* 20: 2888–2894. <https://doi.org/10.1002/chem.201304556>
165. Xing H, Wei T, Lin X, Dai Z (2018) Near-infrared MnCuInS/ZnS@BSA and urchin-like Au nanoparticle as a novel donor-acceptor pair for enhanced FRET biosensing. *Anal Chim Acta* 1042:71–78. <https://doi.org/10.1016/j.aca.2018.05.048>
166. Zhang R, Sun J, Ji J et al (2019) A novel “OFF-ON” biosensor based on nanosurface energy transfer between gold nanocrosses and graphene quantum dots for intracellular ATP sensing and tracking. *Sensors Actuators, B Chem* 282:910–916. <https://doi.org/10.1016/j.snb.2018.11.141>
167. Qaddare SH, Salimi A (2017) Amplified fluorescent sensing of DNA using luminescent carbon dots and AuNPs/GO as a sensing platform: A novel coupling of FRET and DNA hybridization for homogeneous HIV-1 gene detection at femtomolar level. *Biosens Bioelectron* 89:773–780. <https://doi.org/10.1016/j.bios.2016.10.033>
168. Wang Y, Gan N, Zhou Y et al (2017) Novel single-stranded DNA binding protein-assisted fluorescence aptamer switch based on FRET for homogeneous detection of antibiotics. *Biosens Bioelectron* 87:508–513. <https://doi.org/10.1016/j.bios.2016.08.107>
169. Yu M, Wang H, Fu F et al (2017) Dual-Recognition Förster Resonance Energy Transfer Based Platform for One-Step Sensitive Detection of Pathogenic Bacteria Using Fluorescent Vancomycin-Gold Nanoclusters and Aptamer-Gold Nanoparticles. *Anal Chem* 89:4085–4090. <https://doi.org/10.1021/acs.analchem.6b04958>
170. Han Z, Chen L, Weng Q et al (2018) Silica-coated gold nanorod@CdSeTe ternary quantum dots core/shell structure for fluorescence detection and dual-modal imaging. *Sensors Actuators B Chem* 258:508–516. <https://doi.org/10.1016/j.snb.2017.11.157>
171. Ye T, Peng Y, Yuan M et al (2019) A “turn-on” fluorometric assay for kanamycin detection by using silver nanoclusters and surface plasmon enhanced energy transfer. *Microchim Acta* 186(40). <https://doi.org/10.1007/s00604-018-3161-3>
172. Léger C, Di Meo T, Aumont-Nicaise M et al (2019) Ligand-induced conformational switch in an artificial bidomain protein scaffold. *Sci Rep* 9(1178). <https://doi.org/10.1038/s41598-018-37256-5>
173. Wu Y-T, Qiu X, Lindbo S et al (2018) Quantum Dot-Based FRET Immunoassay for HER2 Using Ultrasmall Affinity Proteins. *Small* 14:1802266. <https://doi.org/10.1002/smll.201802266>

Publisher's note Springer Nature remains neutral with regard to jurisdictional claims in published maps and institutional affiliations.